Dual control of cardiac Na^+–Ca^{2+} exchange by PIP_2: electrophysiological analysis of direct and indirect mechanisms

Alp Yaradanakul[1], Siyi Feng[1], Chengcheng Shen[1], Vincenzo Lariccia[1], Mei-Jung Lin[1], Jinsong Yang[1], Kang T. M.[1], Ping Dong[1], Helen L. Yin[1], Joseph P. Albanesi[2] and Donald W. Hilgemann[1]

Departments of [1]Physiology and [2]Pharmacology, University of Texas Southwestern Medical Center at Dallas, Dallas, TX 75390, USA

Cardiac Na^+–Ca^{2+} exchange (NCX1) inactivates in excised membrane patches when cytoplasmic Ca^{2+} is removed or cytoplasmic Na^+ is increased. Exogenous phosphatidylinositol-4,5-bisphosphate (PIP_2) can ablate both inactivation mechanisms, while it has no effect on inward exchange current in the absence of cytoplasmic Na^+. To probe PIP_2 effects in intact cells, we manipulated PIP_2 metabolism by several means. First, we used cell lines with M1 (muscarinic) receptors that couple to phospholipase C's (PLCs). As expected, outward NCX1 current (i.e. Ca^{2+} influx) can be strongly inhibited when M1 agonists induce PIP_2 depletion. However, inward currents (i.e. Ca^{2+} extrusion) without cytoplasmic Na^+ can be increased markedly in parallel with an increase of cell capacitance (i.e. membrane area). Similar effects are incurred by cytoplasmic perfusion of GTPγS or the actin cytoskeleton disruptor latrunculin, even in the presence of non-hydrolysable ATP (AMP-PNP). Thus, G-protein signalling may increase NCX1 currents by destabilizing membrane cytoskeleton–PIP_2 interactions. Second, to increase PIP_2 we directly perfused PIP_2 into cells. Outward NCX1 currents increase as expected. But over minutes currents decline substantially, and cell capacitance usually decreases in parallel. Third, using BHK cells with stable NCX1 expression, we increased PIP_2 by transient expression of a phosphatidylinositol-4-phosphate-5-kinase (hPIP5KIβ) and a PI4-kinase (PI4KIIα). NCX1 current densities were decreased by > 80 and 40%, respectively. Fourth, we generated transgenic mice with 10-fold cardiac-specific overexpression of PI4KIIα. This wortmannin-insensitive PI4KIIα was chosen because basal cardiac phosphoinositides are nearly insensitive to wortmannin, and surface membrane PI4-kinase activity, defined functionally in excised patches, is not blocked by wortmannin. Both phosphatidylinositol-4-phosphate (PIP) and PIP_2 were increased significantly, while NCX1 current densities were decreased by 78% with no loss of NCX1 expression. Most mice developed cardiac hypertrophy, and immunohistochemical analysis suggests that NCX1 is redistributed away from the outer sarcolemma. Cholera toxin uptake was increased 3-fold, suggesting that clathrin-independent endocytosis is enhanced. We conclude that direct effects of PIP_2 to activate NCX1 can be strongly modulated by opposing mechanisms in intact cells that probably involve membrane cytoskeleton remodelling and membrane trafficking.

(Resubmitted 18 March 2007; accepted after revision 24 May 2007; first published online 31 May 2007)
Corresponding author D. W. Hilgemann: Department of Physiology, UTSouthwestern Medical Center, Dallas, TX 75390-9040, USA. Email: donald.hilgemann@utsouthwestern.edu

PIP_2 is the lipid precursor of three second messengers, inositol 1,4,5-trisphosphate (IP_3), diacylglycerol (DAG), and phosphatidyl inositol 3,4,5-trisphosphate (PIP_3) (Tolias & Cantley, 1999). In addition, it participates directly in many signalling pathways and cellular processes (Downes *et al.* 2005). It interacts with and modulates the function of membrane-associated cell signalling proteins, membrane cytoskeletal proteins (Yin & Janmey, 2003), and multiple proteins involved in endocytosis (Czech, 2003) as well as exocytosis (Grishanin *et al.* 2004; Milosevic *et al.* 2005). In addition, the activities of many ion transporters and channels are profoundly affected by PIP_2 (Hilgemann *et al.* 2001; Suh & Hille, 2005). Whether PIP_2 is acting as a bonafide second messenger must be answered on a case-by-case basis. For the potassium channels that mediate 'M-currents' of sympathetic neurons (Haley

 DOI: 10.1113/jphysiol.2007.132712

et al. 1998; Suh & Hille, 2002), receptor-activated PLC activities appear to physiologically control ion channels via PIP_2 depletion (Suh & Hille, 2005). For the classical inward rectifier potassium channels, however, PIP_2 affinity is so high that nearly total PIP_2 depletion would be necessary to affect channel activity (Soom *et al.* 2001). The role of PIP_2 at other ion channels and transporters is presently controversial, and this article focuses on the cardiac Na^+–Ca^{2+} exchanger (NCX1).

The cardiac Na^+–Ca^{2+} exchanger (NCX1), like most potassium channels, does not have a specific PIP_2 requirement for activity, but rather a general requirement for anionic phospholipids (Hilgemann *et al.* 2001). That PIP_2 plays a physiologically unique role is supported by evidence that PIP_2 synthesis underlies activation of NCX1 by cytoplasmic ATP in cardiac membranes (Hilgemann & Ball, 1996). Also, it has been demonstrated that PIP_2 is bound physiologically by the cardiac exchanger (Asteggiano *et al.* 2001). Nevertheless, the functional role that PIP_2 is playing physiologically remains largely enigmatic. G-protein-coupled receptor activation usually does not lead to PIP_2 depletion in cardiac muscle (Nasuhoglu *et al.* 2002*a*). It is proposed that highly localized PIP_2 depletions can occur during receptor activation in cardiac myocytes, and that such depletions serve to signal from specific receptors to specific PIP_2-sensitive potassium channels (Cho *et al.* 2005). However, we are aware of no evidence that cardiac Na^+–Ca^{2+} exchangers are inhibited by any receptor pathway in myocytes. In contrast, α-adrenergic (Ballard & Schaffer, 1996; Stengl *et al.* 1998) and endothelin (Zhang *et al.* 2001)-coupled pathways appear to activate, not inhibit, exchange activity.

In this light, a second perspective on PIP_2 appears relevant. PIP_2 synthesis occurs mostly at the cell surface, and the sparsity of PIP_2 on internal membranes will inhibit PIP_2-activated channels and transporters during their processing and trafficking. This general inhibitory mechanism might be important to maintain ion homeostasis in the secretory pathway during the processing and trafficking of channels and transporters (Hilgemann *et al.* 2001). Ca^{2+} homeostasis in both the endoplasmic reticulum and Golgi membrane system (Van *et al.* 2004; Vanoevelen *et al.* 2005; Ramos-Castaneda *et al.* 2005) would presumably be disrupted by reverse mode exchange activity, if NCX1 were active during its trafficking.

Another reason for enigma about the role of PIP_2 for NCX1 is that PIP_2 metabolism couples to innumerable signalling pathways. Loss of PIP_2 might affect Na^+–Ca^{2+} exchange via multiple indirect mechanisms. Protein kinase C (PKC) can apparently either stimulate or inhibit NCX1 (Iwamoto *et al.* 1998; Zhang *et al.* 2006). NCX1 has high affinity interactions with ankyrin (Li *et al.* 1993; Mohler *et al.* 2005), and in cell lines both the activity and localization of NCX1 appear to depend on actin cytoskeleton (Condrescu & Reeves, 2006). Na^+–Ca^{2+} exchangers have recently been suggested to move in and out of the cardiac surface membrane more frequently than expected from total protein half-life (Egger *et al.* 2005). The exchanger has a putative endocytosis motif (YCH) close to its C-terminus (Linck *et al.* 1998), and it is suggested to interact with caveolins that may take part in clathrin-independent membrane trafficking (Bossuyt *et al.* 2002). While recent work suggests that PLC signalling can be localized to 'lipid rafts' in myocytes (Morris *et al.* 2006), the caveolin interaction is disputed (Cavalli *et al.* 2007). In any case, there is wide agreement that PIP_2 synthesis recruits endocytic proteins to the surface membrane and promotes the final stages of endocytosis (Haucke, 2005). In this article, we describe initial evidence that enhanced PIP_2 levels in intact cells can promote the internalization of NCX1. This evidence is based on manipulating PIP_2 and its metabolism in parallel with measurements of cell area by high resolution capacitance recording, and biochemical evidence for this same conclusion is presented in the following article (Shen *et al.* 2007).

Methods

All animal protocols used in this study were approved by the University of Texas Southwestern Institutional Animal Care and Use Committee. Animals were killed by I.P. injection of Euthasol (Virbac, AH, Inc.), 100 mg (kg body weight)$^{-1}$ and hearts were excised only after cessation of paw-pinch reflexes.

Cells and transfections

Cell cultures were maintained as described (Linck *et al.* 1998). For patch clamp, cells were detached with 0.25% trypsin in divalent-free solution for 3 min, resuspended, and used within 10 h. Lipofectamine 2000 (Invitrogen, Carlsbad, CA, USA) was used for transient transfections of cDNA. Myocytes were isolated as described (O'Connell *et al.* 2003) and used within 10 h. During, this time the myocytes were maintained in the normally Ca^{2+} free perfusion solution. The cDNA construct for green fluorescent protein (GFP) fused with a PLCδ pleckstrin homology (PH) domain (GFP-PH domain; Stauffer *et al.* 1998) was provided by Tobias Meyer (Stanford). The baby hamster kidney (BHK) cell line expressing NCX1 was provided by Kenneth D. Philipson (UCLA). A Chinese hamster ovary (CHO) cell line expressing hM1 receptors (Selyanko *et al.* 2000) and cDNA for the hM1 receptor were provided by Mark S. Shapiro (University of Texas at San Antonio). A human embryonic kidney (HEK 293) cell line expressing Kir6.2 with SUR2A (i.e. cardiac K_{ATP} channels) with G418 (Life Technologies, Inc.) and Zeocin (Invitrogen) selection was provided by Andrew Tinker (University College, London, UK). A

Table 1. Solution compositions (mM)

	C1	X1	C2	X2	C3	X3	C4	X4	C5	X5	C6	X6	C7	X7
NMDG	60	100	80	—	30	90	—	—	—	—	—	—	—	100
TEA	20	20	40	20	30	20	20	20	—	—	20	40	—	—
NaOH	[40]	20	—	120	40	20	0	[120]	—	120	12	120	[–]	—
LiOH	—	—	—	—	—	—	110	[120]	—	0	—	—	—	—
KOH	—	—	—	—	—	—	—	—	120	5	—	—	[110]	5
CsOH	20 [40]	—	20	—	—	—	—	—	100	0	20	5	[110]	—
EGTA	10	0.5	2	2	[20]	—	3	1	1	0	30	—	1	—
Hepes	15	15	15	20	15	15	15	15	10	10	45	15	10	10
$MgCl_2$	0.5	2	0.5	2	0.5	1	0.5	2	0.5	1	1	—	0.5	—
$CaCl_2$	—	2	—	—	—	[2]	2.7	[–]	[–]	2	—	1.2	—	2
$CaCO_3$	[7] [0] [2.1]	—	[0] [1.7]	—	[10]	—	—	—	—	—	25	—	—	—
(Mg)ATP	—	—	—	—	2	[–]	2	—	2	—	2	—	[1]	—
(Mg)GTP	—	—	—	—	0.2	[–]	0.2	—	0.2	—	—	—	—	—

All solutions were adjusted to pH 7.0 with aspartic acid. Brackets ([–])denote concentrations that were changed during experiments.

double NCX1-hM1-expressing BHKl line was generated by transfecting the NCX1-expressing cell line (Linck *et al.* 1998) with pcDNA3.1/hg-hM1 followed by selection with 400 μg ml^{-1} of hygromycin B (Sigma, St Louis, MO, USA).

Patch clamp

Extracellular solutions were changed by moving the pipette tip with the voltage-clamped cell between temperature-controlled solution streams (36°C) with gravity-driven flow through double-barrel square glass tubes (0.6 mm; ∼15 cm solution column restricted by 8 cm lengths of 0.15 mm i.d. tubing). Four solution lines were available in the chamber employed. Pipette perfusion was essentially as previously described (Lu *et al.* 1995) via flexible quartz capillaries (109 μm o.d., 40 μm i.d.; PolymicoTechnologies, Phoenix, AZ, USA) to deliver cytoplasmic solution to a position within 50 μm of the cell opening. The capillary tip was positioned within the patch pipette with a one-dimensional hydraulic manipulator. Based on current measurements, the ionic composition of cytoplasmic solution could be exchanged within 10 s upon starting solution delivery (Lu *et al.* 1995), and the positive pressure required was without consequence for electrical recording.

Axopatch 200B and 1C patch clamps were employed. For capacitance recording, patch pipettes were coated with melted dental wax (Kerr 00623; Romulus, MI, USA) and cut (Hilgemann & Lu, 1998) to obtain 4–7 μm i.d. tips with thick walls (0.2–0.6 MΩ). Seals were 3–10 GΩ, cell resistance was typically 30–100 MΩ, and cell time constants were < 150 μs. Capacitance was monitored with phase-lock amplifiers via sinusoidal voltage oscillations (20–40 mV) at 480–530 Hz (Lu *et al.* 1995). Upon establishing giga-seals in on-cell configuration, capacitance transients were compensated via the fast compensation controls. After rupture of the patch membrane, the whole-cell capacitance was optimally compensated. The phase-lock angle was then determined at which small changes of capacitance compensation had no influence on the phase-lock output. In the majority of recordings, phase-lock angles for capacitance recording were less than 10 deg different from those obtained for a 20 pF capacitor with no series resistance. It was routinely verified that substantial conductance changes had negligible effects on capacitance records. Also of note is that most capacitance changes described in Results occurred with little or no change of the inferred cell conductance.

Solutions and chemicals

Table 1 gives the composition (mM) of the solutions employed in patch-clamp experiments. 'C' and 'X' indicate solutions used on the cytoplasmic and extracellular membrane sides, respectively. pH of all solutions was adjusted to 7.0 with L-aspartate. Chloride conductances were minimized by using solutions with 5 mM or less chloride. 'WEBMAXC EXTENDED' (http://www.stanford.edu/∼cpatton/webmaxc/webmaxcE.htm) was used to calculate free Ca^{2+} concentrations. When $CaCO_3$ was employed, solutions were heated to 80°C and bubbled with N_2 for 20 min to remove CO_2. Stock solutions of ATP and adenosine 5′-(β,γ-imido) triphosphate (AMP-PNP) were prepared as Mg salts and free acid of the nucleotides in a ratio of 4 : 1 to preserve free Mg^{2+} at 0.5 mM in cytoplasmic solutions. Unless indicated otherwise, all

chemicals were from Sigma and were the highest purity grade available.

Transgenic mice

Mice overexpressing PI4KIIα in myocytes were developed as described (Rothermel *et al.* 2001). The cDNA insert for myc-tagged PI4KIIα was cloned into a *Sal* I-digested α-myosin heavy chain promoter (α-MHC). Mice were generated by DNX Transgenic Services (Cranbury, NJ, USA). Founder lines were identified by Southern analysis using a probe for the hGH poly(A) signal sequences and subsequently by PCR using primers for the region of α-MHC to the myc-tag. Animals were genotyped by Southern blot of tail genomic DNA.

Western blotting

Hearts isolated as described above were perfused for 1 min, snap-frozen, and powdered in liquid nitrogen. The powder was suspended in ice-cold buffer (150 mM NaCl, 1 mM EDTA, 1 mM EGTA, 50 mM Tris (pH 7.4), 0.5% Triton X-100) with protease inhibitors (Roche) and after 15 min cleared by centrifugation at 14 000 *g* for 5 min at 4°C. Equal protein amounts (80 μg by the Bradford method) were subjected to SDS-PAGE and transferred to nitrocellulose membranes. Immunoblots were probed with anti-PI4KIIα (Wang *et al.* 2003) or anti-myc, followed by horseradish peroxidase-conjugated anti-rabbit IgG or anti-mouse IgG, respectively. Protein was visualized by enhanced chemi-luminescence (ECL, Amersham).

Lipid analysis and assays

Anionic phospholipids were measured in duplicate (Nasuhoglu *et al.* 2002*b*). Cardiac membranes were prepared with protease inhibitors (Nasuhoglu *et al.* 2002*b*) from myocytes. Lipid kinase (30°C) and phosphatase (37°C) activities (Nasuhoglu *et al.* 2002*b*) were measured in 300 mM sucrose, 100 mM NaCl, 10 mM Hepes, 4 mM EGTA, 0.5 mM $MgCl_2$ and 0.1% Triton X-100 at pH 7.0 (Nasuhoglu *et al.* 2002*b*).

Histological analysis

After 5 min perfusion with Ca^{2+}-free solution, hearts were fixed overnight in 10% formalin at 4°C. Samples were dehydrated, mounted in paraffin, sectioned and stained with either eosin and haematoxylin dyes to determine cell and nuclear size or Masson trichrome dye to visualize collagen deposits (Rothermel *et al.* 2001).

Membrane traffic assays

Myocytes were isolated and plated onto cover slips (O'Connell *et al.* 2003) that were transferred for 10 min into CO_2-equilibrated solution without serum and then to solutions with membrane markers for the times given in Results: 20 μg ml^{-1} Alexafluor-labelled transferrin (Molecular Probes, Eugene, OR, USA), 0.5 μg ml^{-1} FITC-labelled cholera toxin B subunit (Sigma), or 6 μM AM 1-43 (Biotium, Hayward, CA, USA). Cells were washed at 4°C for 1 min, fixed in 1% formaldehyde for 10 min, washed with PBS, and exposed to 50 mM NH_4Cl for 10 min. A live-cell fluorescence assay was used to follow uptake and release of membrane markers. Myocytes were incubated with fluorescent probes at 37°C for the times given in Results and were diluted into marker-free culture medium with the hydrophobic quencher, SCAS (20 μM; Biotium) in a temperature-controlled chamber on a Nikon TE2000 inverted microscope. Whole-myocyte fluorescence was monitored (CoolSnap HQ) as soon as myocytes settled. After an initial rapid fluorescence decline over 2 min, which reflects quenching and loss of surface-bound marker, fluorescence decreased over 20–50 min to nearly the level of myocyte autofluorescence. Exposure frequency selected was low enough (0.2–0.05 Hz) for photobleaching to be negligible. The slow decline phase is therefore assumed to reflect release of marker to the extracellular medium via membrane recycling.

Immunohistochemistry and confocal microscopy

Freshly isolated myocytes were fixed as just described and labelled with polyclonal anti-PI4KIIα rabbit antibody (Wang *et al.* 2003) or monoclonal NCX1 antibody (Frank *et al.* 1992) as follows. After PBS rinse, cells were permeablized with 0.1% Triton X-100 for 10 min and then washed with PBS. They were then preblocked in PBS containing 10% donkey serum with 3% bovine serum albumin for 1 h. Anti-PI4KIIα or anti-NCX1, R3F1 (Frank *et al.* 1992), was added at 1 : 20 and 1 : 100 dilutions in fresh solution containing 20% preblock solution and 80% PBS, and cells were incubated for an additional 2 h. Then, cells were washed 3 times for 10 min with incubation solution. Anti-rabbit or anti-mouse FITC-conjugated secondary antibody was added at 1 : 50 and 1 : 100 for 45 min, and cells were again washed 3 times for 10 min with PBS. Images were collected on a Zeiss 510 laser scanning confocal microscope, using a ×63 1.3 NA PlanApo objective, and images were analysed using Metamorph and Scion Image software. Live-cell imaging under patch clamp was carried out with a Nikon EZ-C1 scanning confocal microscope system with a ×60 1.45 NA objective.

Statistical analysis

Numbers in figures refer to numbers of hearts for biochemical measurements and numbers of myocytes

for fluorescence measurements. Error bars give standard errors of the mean. Symbols indicating significance levels using Student's t test are as follows: $^{*}P < 0.05$, $^{**}P < 0.01$ and $^{***}P < 0.001$.

Results

PIP_2 in excised patches

Figure 1 describes the effects of exogenous PIP_2 on Na^+–Ca^{2+} exchange currents in excised patches from murine myocytes (Fig. 1*A*) and from BHK cells (Fig. 1*B* and *C*). Figure 1*A* and *B* shows the outward NCX1 current (C1 and X1 solutions with 1 μM free cytoplasmic Ca^{2+}, substituting 40 mM Cs^+ for 40 mM Na^+). In the cardiac patch (Fig. 1*A*) the outward current activated by 40 mM cytoplasmic Na^+ decays by 70% over 15 s to a steady level. Then, current turns off completely when cytoplasmic Ca^{2+} is removed (left record). Typical for more than 10 observations with cardiac patches, after applying 40 μM PIP_2 (right record), peak current is increased by 15%, and inactivation processes are completely ablated so that removal of cytoplasmic Ca^{2+} is without effect. These effects reversed over time courses of many minutes after wash-out of PIP_2. As shown in Fig. 1*B*, the effects of PIP_2 in BHK cell patches were qualitatively similar. The record illustrates that inactivation could be fully ablated in BHK patches, but as shown by the composite data points the outward current decreased on average about 30% upon removal of cytoplasmic Ca^{2+}. The data points are normalized to

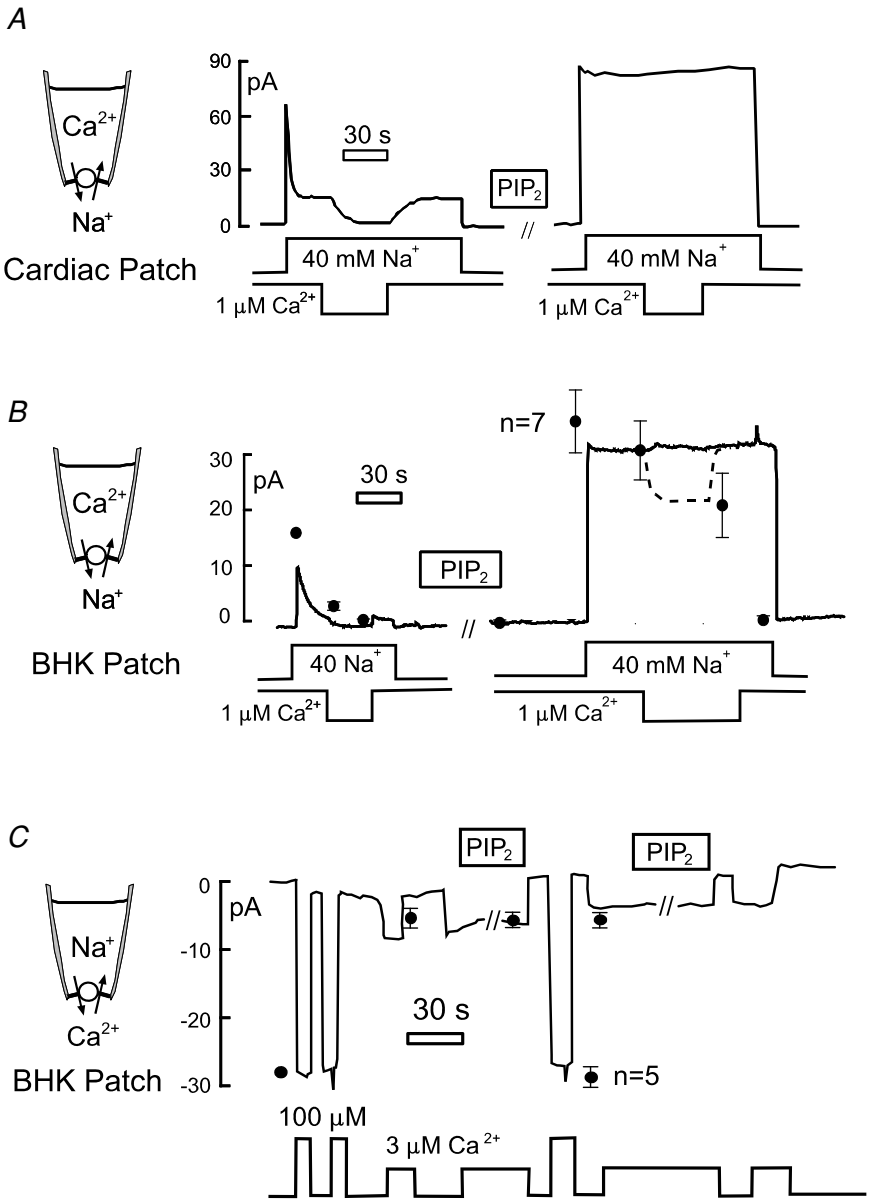

Figure 1. Effects of exogenous PIP_2 (40 μM) on NCX1 currents in excised membrane patches
A, outward exchange current in a mouse myocyte patch. Current is activated by applying Na^+ to the cytoplasmic side (40 mM). Removal of cytoplasmic Ca^{2+} results in complete loss of current. After PIP_2 for 2 min, current does not inactivate and Ca^{2+} removal is without effect. *B*, outward exchange current in a patch from a BHK cell showing similarly complete ablation of exchanger inactivation reactions. Data points give means and standard errors of the mean for 7 equivalent experiments, normalized to the initial peak outward current. *C*, inward exchange current in an excised BHK patch. Current is activated repeatedly by solution with 100 or 3 μM free Ca^{2+}, and application of PIP_2 is without effect. Data points give the means and standard errors of the mean for 5 equivalent experiments normalized to the initial peak inward current.

the initial peak outward current ($n = 7$). As previously described (Collins *et al.* 1992), the secondary requirement for cytoplasmic Ca^{2+} can also be nearly ablated with high ATP concentrations in cardiac patches from myoyctes of some mouse strains.

In contrast to the massive effects of PIP_2 on outward exchange currents, as just described, PIP_2 has no effect on inward exchange current in the absence of cytoplasmic Na^+. Figure 1*C* shows a typical BHK patch record and composite results ($n = 5$) normalized to the initial peak inward current. The inward current was activated by 3 and 100 μM free Ca^{2+}, using 2 mM EGTA to buffer Ca^{2+} in the cytoplasmic solution (C2 and X2 solutions). PIP_2 has no effect on either the submaximal current (3 μM free Ca^{2+}) or the fully activated (100 μM) inward exchange current. Furthermore, numerous interventions known to bind PIP_2 (e.g. neomycin and polylysines) were without effect on the inward current in the absence of cytoplasmic Na^+ (D. W. Hilgemann, unpublished observations). On this basis, we conclude that in excised patches PIP_2 acts only through modulation of the inactivation reactions (Collins *et al.* 1992).

PLC activation in intact cells

To test for the effects of rapidly decreasing PIP_2 via PLC activation, we used a CHO cell line expressing M1 receptors with transient NCX1 expression, and we also used a BHK cell line with stable expression of both NCX1 and M1 receptors, described in Methods. In the CHO cells, PIP_2 mass decreases by 90% within 20 s when receptors are activated by carbachol (Horowitz *et al.* 2005). To identify NCX1-transfected CHO cells and to monitor changes of PIP_2 metabolism, we cotransfected cells with GFP-PH domains (Stauffer *et al.* 1998) that are widely used to monitor PLC activation. C3 and X3 solutions were employed with 1 mM EGTA and 0.5 mM Ca^{2+} (i.e. with 0.5 μM free Ca^{2+}). In the experiment shown in Fig. 2 cell capacitance is initially 35 pF. Exchange current (~80 pA) is activated by switching from an extracellular solution without Ca^{2+} (with 0.2 mM EGTA) to one with 2 mM Ca^{2+}. Application of carbachol (0.2 mM) rapidly inhibits the outward exchange current, and this is accompanied by a small (1.2 pF) rise of capacitance. The rise is then followed by a slow decay over 3 min that corresponds to about 8% of cell area (i.e. 3 pF). The initial increase was absent when 2 mM or more EGTA was included in the pipette solutions, suggesting that it may be caused by internal Ca^{2+} release. The right panel of Fig. 2 illustrates with composite results that the responses of BHK cells expressing both NCX1 and M1 receptors were similar ($n = 16$).

To test whether the inhibition of exchange current involves protein kinases or might be a more direct mechanism (i.e. caused by PIP_2 depletion), we tested whether similar effects occur in the absence of cytoplasmic ATP and the presence of non-hydrolysable ATP (AMP-PNP, 2 mM) in the cytoplasmic solution. Figure 3 shows a typical result. To buffer cytoplasmic Ca^{2+} effectively at 0.5 μM, and thereby ensure that Ca^{2+} transients are not important for the responses, we used large-diameter (4–5 μm) pipette tips with 20 mM EGTA and 10 mM total Ca^{2+} in these experiments. A cell with a strong membrane current response is shown in Fig. 3*A*, and the corresponding GFP-PH domain fluorescence from the central region of the cell is shown in Fig. 3*B*. Accumulation of GFP-PH domain in the cytoplasm mirrors the decrease of exchange current. Profiles of fluorescence across the cell are shown below the fluorescence images in Fig. 3*B*, and Fig. 3*C* shows the average cell fluorescence. Over time, the total GFP-PH domain fluorescence decreases, probably as a result of diffusion into the large-diameter pipette tips employed.

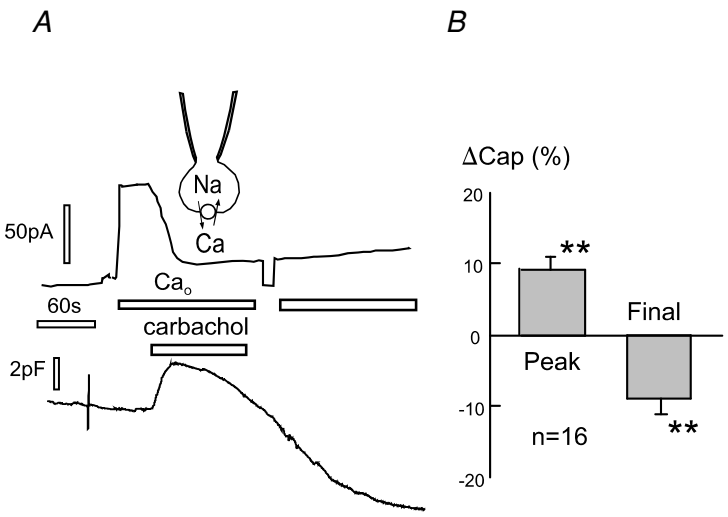

Figure 2. Carbachol (0.2 mM)-induced changes of outward NCX1 current and capacitance in NCX1-hM1-receptor-expressing cells
A, CHO cell expressing NCX1 and M1 muscarinic receptors. Carbachol induces a rapid inhibition of NCX1 current. Cell capacitance rises by 2 pF and then decreases over 4 min by about 8 pF. *B*, composite results for capacitance in 16 equivalent experiments using BHK cells expressing M1 receptors and NCX1.

From these results, we conclude that activation of protein kinases is not required for inhibition of exchange current by muscarinic receptor activation in this model system, and that the likely mechanism is a direct effect of PIP_2 depletion on exchanger function.

We found that the inhibition of outward NCX1 current by carbachol was somewhat variable both in CHO and BHK cells. Strong inhibition of exchange current, defined as a decrease in current greater than 60% within 10 s, was obtained in only 16 of > 50 experiments. This variability of the current response was clearly greater than variability of the capacitance and GFP-PH domain responses, and a possible explanation is that anionic lipids besides PIP_2 can maintain NCX1 in an active state in intact cells.

As described in Fig. 1, PIP_2 activates outward NCX1 current by ablating cytoplasmic Na^+-dependent inactivation, while inward exchange current does not require PIP_2. Therefore, we examined in detail the effects of muscarinic receptor activation on the inward exchange current in the absence of cytoplasmic Na^+ (C4 and X4 solutions), substituting 120 mM Na^+ for 120 mM Li^+ to activate current from the extracellular side with 5.5 μM free Ca^{2+} and no Na^+ on the cytoplasmic side. Figure 4*A* shows the typical result using a BHK cell with stable NCX1 and transient M1 receptor expression. Current decays substantially within 3–20 s, very probably as a result of Ca^{2+} depletion from the cells. After Na^+ was applied and removed twice, carbachol (0.2 mM) was applied in Li^+ solution. Typical for > 15 observations with 4–8 μM free cytoplasmic Ca^{2+}, membrane capacitance initially decreases slightly and then increases by 2–5 pF (i.e. > 10%) over 1–3 min. Within 1 min, inward current activated by extracellular Na^+ was typically doubled. Small increments of capacitance occurring during the application of Na^+ probably reflect a small contribution of NCX1 charge movements to the capacitance signals (Lu *et al.* 1995). With higher cytoplasmic free Ca^{2+} concentrations (not shown), capacitance typically increased within seconds (> 10 observations) of opening the cell, and carbachol was then without effect during the subsequent experiment. This outcome is not unexpected, given the fact that high free Ca^{2+} can substantially activate PLCβs in the absence of Gq activation (Smrcka *et al.* 1991).

Figure 4*B* shows further results for inward exchange current using CHO cells with stable M1 receptor and transient NCX1 and GFP-PH domain expression. On average, the carbachol-induced increase of peak inward current was 62% ($P < 0.01$), while capacitance increased by 7.3%. Next, we tested whether protein kinases are required for these effects. To do so, we performed experiments with non-hydrolysable analogues of both ATP (AMP-PNP, 2 mM) and GTP (GTPγS, 0.2–1 mM). In those experiments, membrane capacitance and inward current spontaneously increased in 1 or 2 min after establishing whole-cell configuration, and carbachol had no further effect. We then tested whether AMP-PNP or GTPγS was the active component of the cytoplasmic solution. It was clearly GTPγS (0.3 mM). As shown in Fig. 4*C*, robust effects of GTPγS (0.3 mM) were obtained in BHK cells perfused initially with AMP-PNP. Cytoplasmic perfusion of GTPγS increased the peak inward exchange currents on average by 111% ($n = 5$; $P < 0.01$) while membrane capacitance increased by 2.5%. These results demonstrate that inward exchange current can probably be activated by G-proteins without hydroysis of ATP, and PLC activation via Gq signalling is a possible pathway.

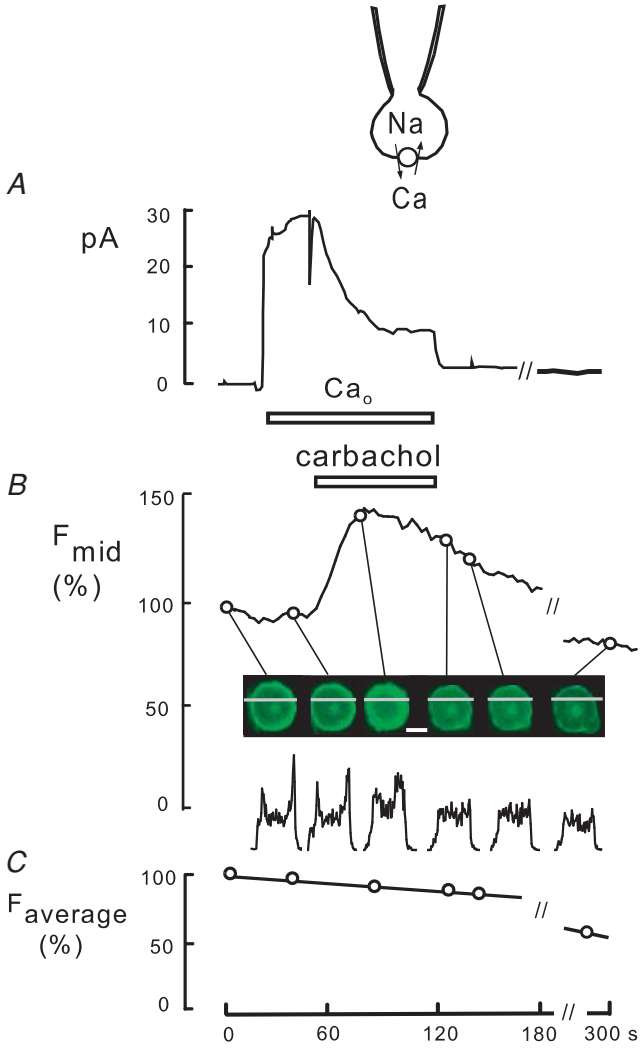

Figure 3. Inhibition of outward NCX1 current by carbachol in a CHO cell expressing M1 muscarinic receptors and GFP-PLCδ-PH domains

The cytoplasm is perfused with non-hydrolysable ATP (AMP-PNP, 2 mM). *A*, outward exchange current. *B*, GFP-PH domain fluorescence. F_{mid} is the average fluorescence of a 4 μm^2 area in the central portion of the cell. Line scans at the times indicated illustrate the usual loss of the PH domain from the membrane in parallel with a gain in the cytoplasm. Calibration bar corresponds to 10 μm. *C*, average total fluorescence ($F_{average}$).

The possibility raised by these experiments is that PIP_2 depletion activates exchange currents without involvement of any ATP hydrolysing mechanism. In addition, disruption of actin cytoskeleton interactions with the membrane is one mechanism consistent with previous studies (Raucher *et al.* 2000). Therefore, we performed experiments to chemically disrupt the cytoskeleton using the same solutions with 2 mM AMP-PNP, and no ATP, in the pipette. After activating inward exchange current multiple times, 0.8 μM latrunculin was perfused into cells to disrupt actin membrane cytoskeleton. While the effect was slower and of smaller magnitude than the effect of GTPγS, latrunculin reliably increased inward currents by 30% over 2 min in parallel with an increase of cell

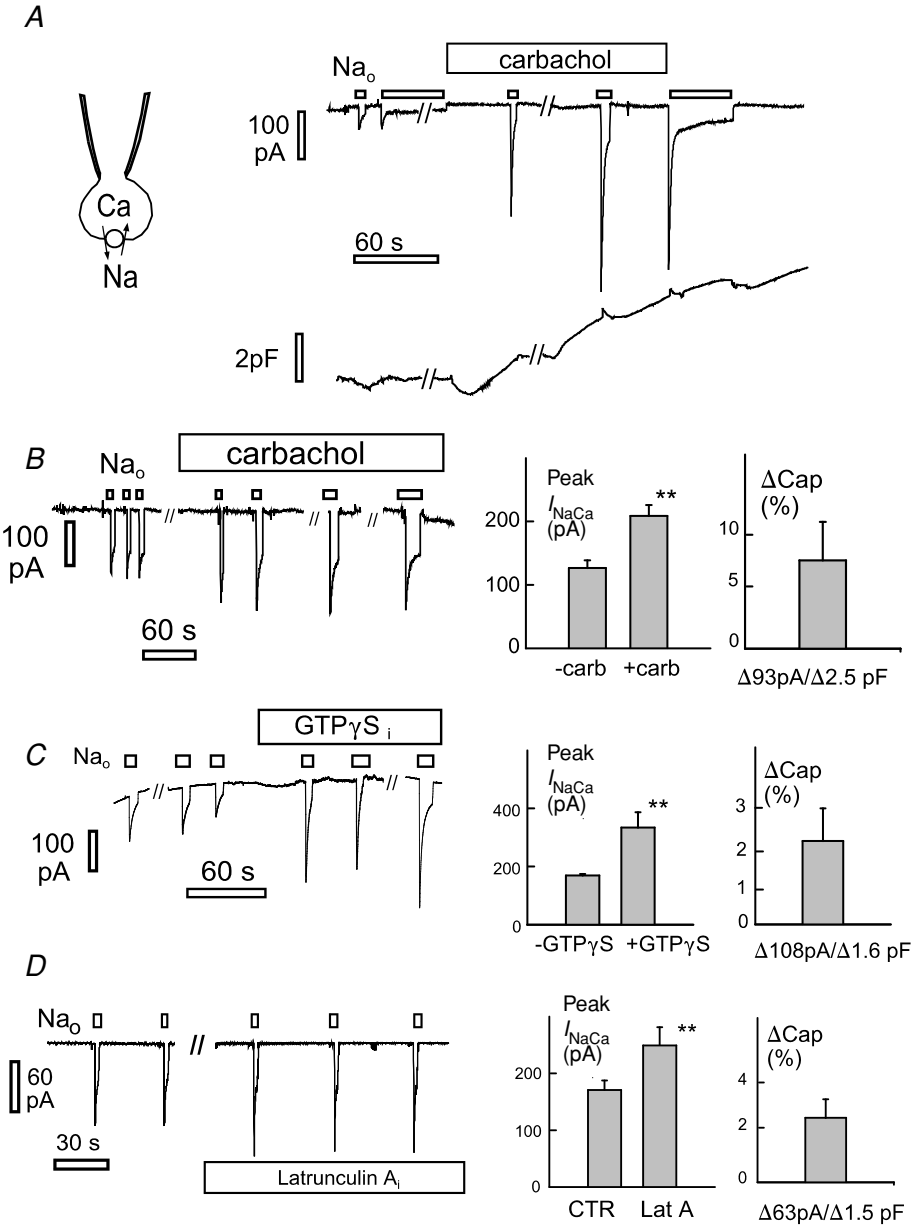

Figure 4. Stimulation of inward NCX1 current by carbachol, GTPγS, and latrunculin in parallel with an increase of capacitance
Right panels, composite results for peak inward current and membrane capacitance. *A*, effect of carbachol (0.2 mM) in a BHK cell expressing NCX1 with transient expression of M1 receptors. *B*, effects of carbachol (0.2 mM) in CHO cells expressing M1 receptors with transient NCX1 expression. *C*, stimulation of inward exchange current by cytoplasm perfusion of GTPγS (0.3 mM) in the presence of AMP-PNP (2 mM). *D*, stimulation of inward exchange current by cytoplasm perfusion of latrunculin (0.8 μM) in the presence of AMP-PNP (2 mM).

capacitance (Fig. 4*D*). Thus, the effects of GTPγS and latrunculin appear qualitatively similar.

PIP_2 perfusion into intact cells

Figure 5 summarizes the results for capacitance recording in which PIP_2 was perfused into multiple cell types via a quartz capillary line brought to within 50 μm of the cell opening (see illustration in Fig. 5*A*). Figure 5*A* shows a typical record from an A9 cell (Clements *et al.* 1976) perfused with a large-diameter pipette tip. The solutions employed in Fig. 5*A* (C5 and X5) approximate physiological saline, except that the cytoplasmic solution was without Ca^{2+}. PIP_2 (40 μM) was perfused into the pipette tip for 3 min, then PIP_2-free solution was perfused into the pipette tip, and the procedure was repeated. Perfusion of PIP_2 resulted in a reduction of cell capacitance by 0.6 pF, about 5% of total cell capacitance, and capacitance returned to baseline within 1–2 min upon removing PIP_2. From $>$ 30 experiments with additional cell types, including CHO and BHK cells, the following observations are reported. The decrease of capacitance with PIP_2 perfusion ranged between 3 and 15% of total cell membrane capacitance. Application of the same liposomes to excised giant patches had no effect or caused a slight increase of membrane capacitance. The effects in cells were typically reversible within 2 or 3 min, and effects were more pronounced when freshly sonicated PIP_2 liposomes were employed, rather than liposomes that had been frozen. After whole-cell recording was established, the ability of PIP_2 to cause a decrease of capacitance was lost within 15 min, presumably because soluble factors necessary for endocytosis were lost from the cells. Other lipids tested in similar experiments did not cause a decrease of cell capacitance. Of most interest to this study, neither dioctanoyl glycerol (100 μM) nor 1-oleoyl-2-acetyl-*sn*-glycerol (100 μM; Avanti Polar Lipids, Alabaster, AL, USA) caused a decrease of capacitance when perfused into BHK cells in the absence of cytoplasmic Ca^{2+}.

The effects of perfusion of PIP_2 on exchange currents are shown in Fig. 5*B* and *C*. In Fig. 5B, outward exchange current and capacitance are recorded simultaneously in a BHK cell expressing NCX1 (C3 and X3 solutions with 20 mM EGTA/10 mM Ca^{2+}). The outward exchange current was activated twice by applying 2 mM extracellular Ca^{2+}. The current (0.2 nA peak) decayed about 30% over 30 s. Small capacitance changes on changing extracellular Ca^{2+} probably reflect a small contribution of transport reactions to the capacitance signal (Lu *et al.* 1995). When PIP_2 (40 μM) was introduced, NCX1 current doubled in 40 s and then decreased by 70% over 3 min. Capacitance began to decrease soon after PIP_2 was applied, and then current and capacitance decreased in parallel. The capacitance decrease (1.2 pF) amounts to 10% of total cell capacitance (11 pF). Peak NCX1 current is decreased by 50% in comparison to initial current.

Figure 5*C* shows exchange currents with nearly physiological Na^+ and Ca^{2+} ion gradients (C6 and X6 solutions with 1.2 μM free Ca^{2+}). The NCX1 current is defined by applying and removing extracellular nickel (Ni^{2+}, 4 mM). The current amounts to -28 pA at 0 mV, and current–voltage (*I–V*) relations show reversal at about +30 mV. When PIP_2 is perfused into the cell, inward current increases briefly and then declines by $>$ 80% over 90 s. After removal of PIP_2, current recovers to 80% of initial current. The inset in Fig. 5*C* shows *I–V* relations defined by subtracting currents, as indicated in the current record. The baseline *I–V* with extracellular Ni^{2+} was very stable, while the current inhibited by Ni^{2+} was almost abolished in the presence of PIP_2.

Lipid kinase overexpression in BHK cells

To address the effects of PIP_2 metabolism with molecular biological approaches, we carried out experiments to determine how Na^+–Ca^{2+} exchange currents are modified by overexpressing lipid kinases. Lipofectamine-mediated transfections were carried out with BHK cells expressing NCX1, and cotransfection of GFP was used to identify transfected cells. Three PI4-kinases (human IIα, IIβ and IIIβ) and three PIP5-kinases (human Iα, Iβ and Iγ-short) were tested. In addition, the PI4KIIα was prepared as an adenovirus and employed with the BHK cell line expressing NCX1 and finally, similar experiments were performed in HEK 293 cells in which NCX1 was transfected together with GFP and one lipid kinase. Exchange currents were analysed in both excised giant patches and in whole-cell recordings.

In excised giant patches, we analysed the kinetics of inactivation of outward exchange currents and the stimulatory effects of cytoplasmic ATP that are thought to reflect lipid kinase activity. In no case was the NCX1 current density in excised patches significantly increased, and in no case was the stimulatory effect of ATP on exchange current in excised patches significantly increased in magnitude or rate. A significant complication in these experiments was that effects of ATP on the outward exchange current, in excised patches, were generally small and variable. Overexpression of hPIP5KIα actually caused a significant decrease of the normalized stimulation of exchange current in excised patches by cytoplasmic ATP (data not shown), as expected for a dominant negative effect. We also note that results of using siRNA approaches to knock down lipid kinases were not significant for exchange currents in these protocols.

Figure 6 summarizes significant data for overexpression of lipid kinases using whole-cell recording to characterize

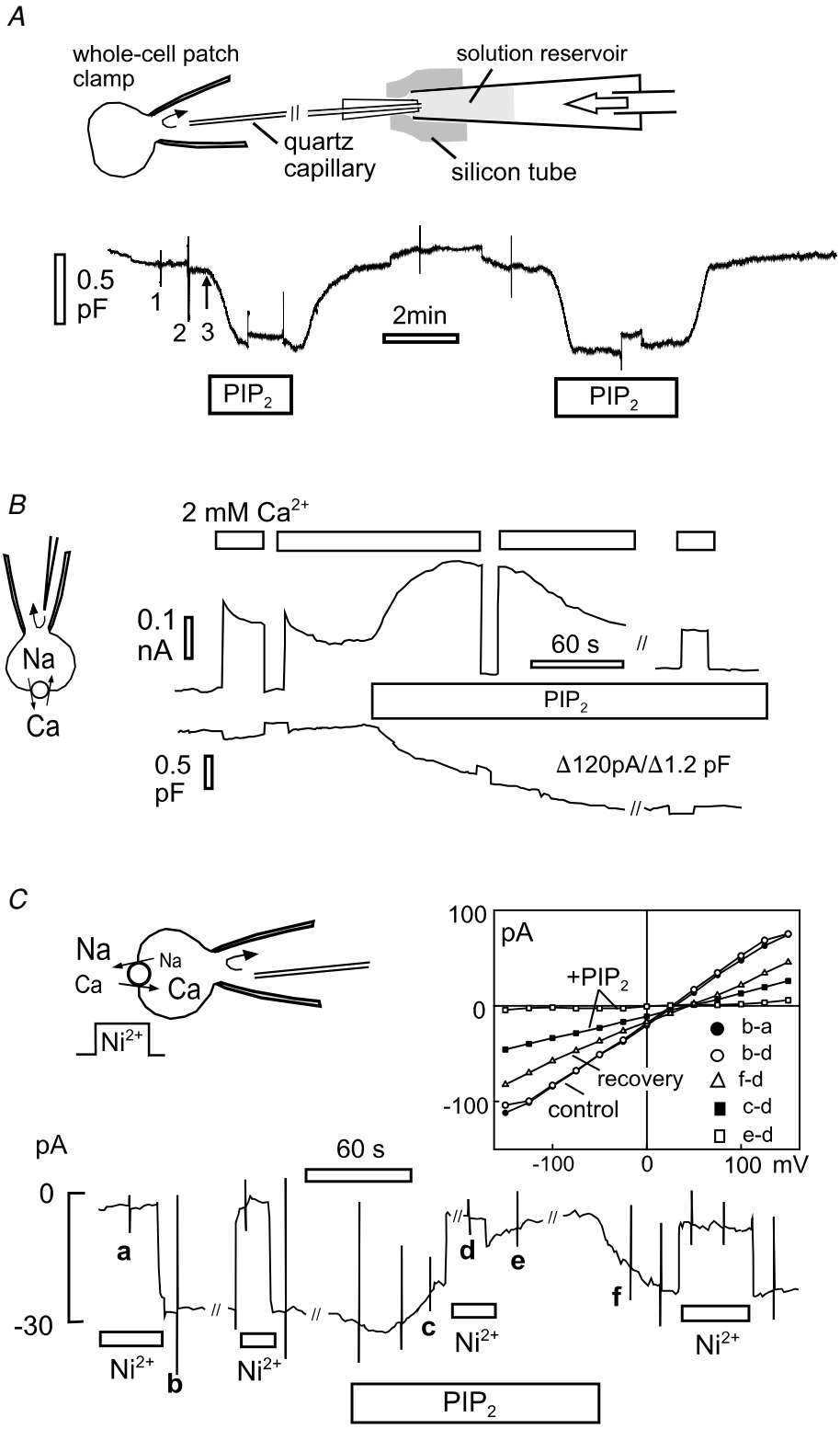

Figure 5. Capacitance and NCX1 current changes associated with perfusion of PIP_2 into cells in whole-cell voltage clamp

A, illustration of pipette perfusion method and the reversible effects of perfusing PIP_2 (40 μM) into an A9 cell. Solutions are changed by removing (1) and attaching (2) solution reservoirs (10–50 μl) to a quartz capillary through a silicon sleeve and applying positive air pressure to the reservoir (3). The decrease of capacitance (0.6 pF) corresponds

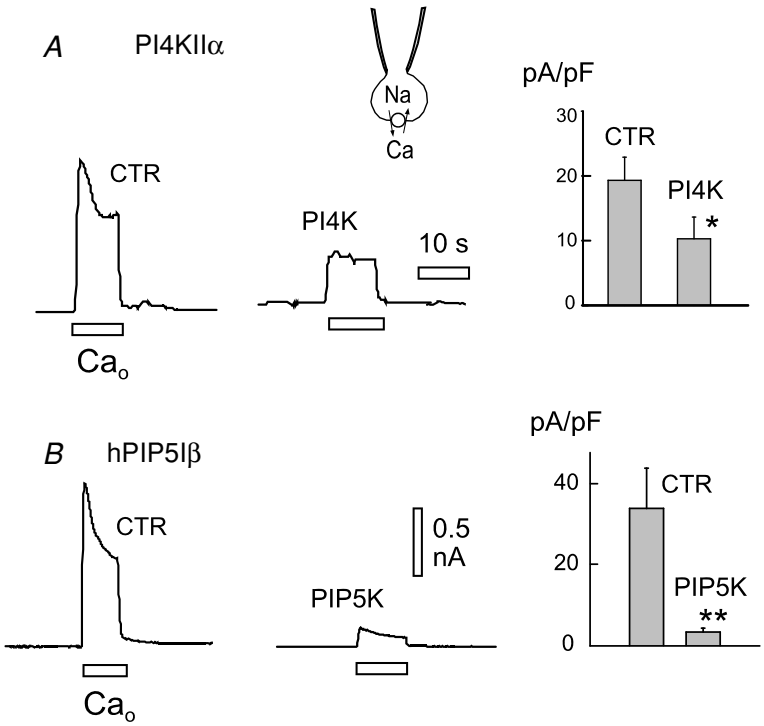

Figure 6. Effects of overexpressing PI4KIIα and hPIP5KIβ on outward exchange currents in whole-cell recordings of outward exchange current in BHK cells
A, typical current records (left) and composite results (right) for 5 control and 5 PI4KIIα cells. *B*, typical current records (left) and composite results (right) for 7 control and 7 PIP5KIβ cells.

exchange currents (C3 and X3 solutions with 20 mM EGTA/10 mM Ca^{2+}). In short, the outward exchange current was significantly decreased by overexpression of multiple lipid kinases, and in no case was whole-cell current increased. As shown in Fig. 6*A*, overexpression of the type IIα PI4-kinase was associated with a decrease of peak outward exchange current by 45% ($n = 5/5$) in excised patches. As shown in Fig. 6B, overexpression of human type Iβ PIP5-kinase was associated with a decrease of peak outward exchange current by about 85% ($n = 7/7$).

Failure of wortmannin to block activation of NCX1 and K_{ATP} channels by ATP in excised patches

To better define how phosphoinositides may affect NCX1 function in a cardiac environment, we decided to generate mice with cardiac α-myosin heavy chain (MHC)-driven overexpression of a lipid kinase. We chose to express a PI4-kinase, rather than a PIP-kinase, because previous work suggested that, in giant excised cardiac patches, phosphorylation of PI to PIP may be rate-limiting in PIP_2 generation upon application of ATP (Hilgemann & Ball, 1996). Mammalian cells express two classes of PI4-kinase, termed types II and III, and each class contains α- and β-isoforms (Balla & Balla, 2006). The type III kinases are inhibited by micromolar concentrations of wortmannin, whereas the type II kinases are insensitive to wortmannin (Barylko *et al.* 2001). In intact cells, wortmannin blocks the recovery of PIP_2-activated currents after PIP_2 has been depleted by activation of PLCs (Suh & Hille, 2002; Cho *et al.* 2005) in support of an important role for type III PI4-kinases for maintained PLC signalling (Nakanishi *et al.* 1995).

To decide whether to select a type II or type III kinase to overexpress in hearts we examined the effects of wortmannin on the stimulation of NCX1 and K_{ATP} potassium channel currents by ATP in cardiac patches. Figure 7*A* documents our routine observation ($n > 10$) that the stimulation of NCX1 and K_{ATP} potassium channel currents by cytoplasmic ATP cannot be blocked by wortmannin. For illustration purposes, Fig. 7*A* shows results from a murine myocyte patch using a protocol to determine effects at both Na^+–Ca^{2+} exchange and K_{ATP}

to 5% of the cell capacitance. *B*, effects of perfusing PIP_2 into a BHK cell expressing NCX1. Outward exchange current is activated by applying 2 mM Ca^{2+} on the extracellular side. With PIP_2 perfusion (40 μM), current increases briefly and then decreases over 2 min in parallel with a 12% decrease of membrane capacitance. *C*, PIP_2 inhibition of NCX1 currents with physiological ion gradients. Exchange current is defined by application and removal of 4 mM Ni^{2+} in the extracellular solution. *I–V* relations were taken at points marked a–f. Plots are given for subtracted *I–V*s at the start of the experiment (b – a and b – d), during perfusion of PIP_2 (c – d and e – d), and after removal of PIP_2 (f – d).

currents. A high concentration (3 μM) of wortmannin is present in all solutions (C7 and X7). The pipette contains Ca^{2+} (2 mM), low K^+ (5 mM) and no K^+ channel blockers. Outward Na^+–Ca^{2+} exchange current is activated first by applying 40 mM Na^+ from the cytoplasmic side in exchange for 40 mM Cs^+. Exchange current inactivates partially, as usual, over 20 s. Thereafter, the cytoplasmic solution was switched to one containing 140 mM K^+, thereby activating a very small outward current. Then, during application of ATP (2 mM) to the cytoplasmic side, current increases with a half-time of 12 s. This time course is typical for more than 50 observations, and the average value in published data (Hilgemann & Ball, 1996) was 11.8 ± 3.5 s ($n = 4$). Upon removal of ATP current, the direct inhibitory effect of ATP is released and current increases 3.3-fold, thereby revealing the large magnitude of the stimulatory effect of ATP on the K_{ATP} channels. This compares to an average from published records of 4.2 ± 0.46 fold. After applying and removing ATP again, the Na^+–Ca^{2+} exchange current is activated with

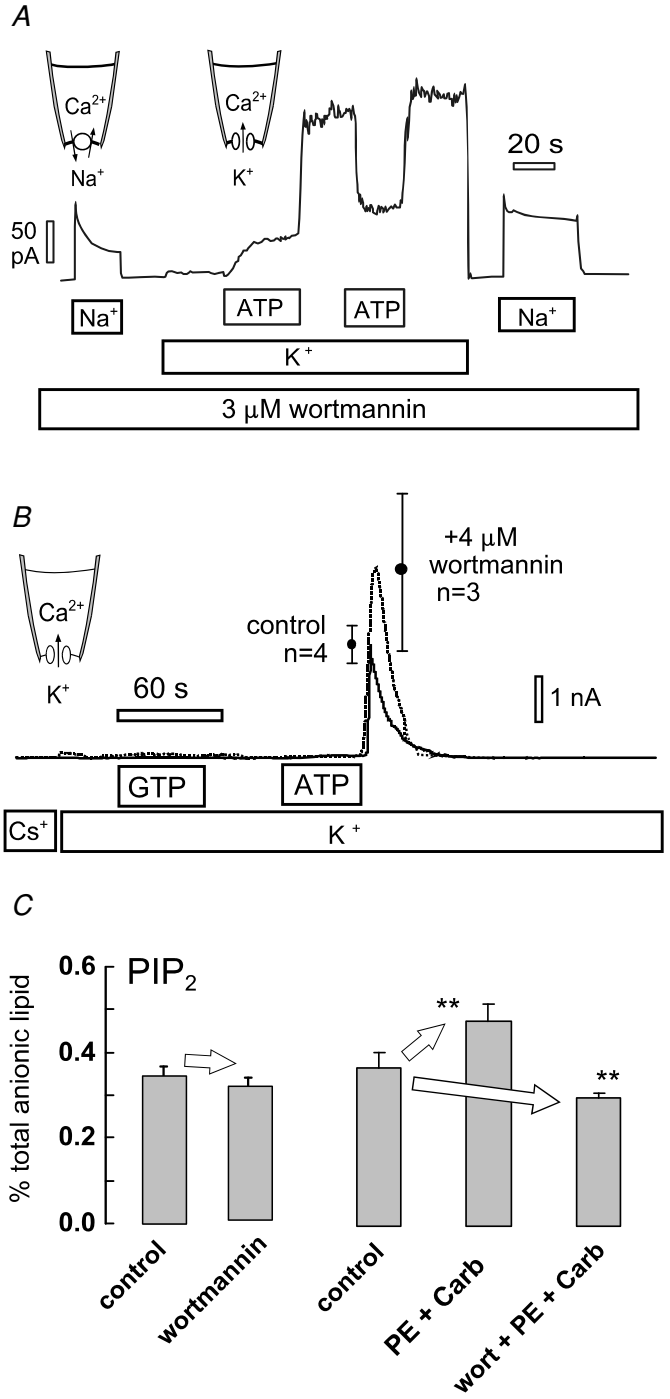

Figure 7. Tests for the wortmannin sensitivity of PIP_2-sensitive currents and cardiac PIP_2 metabolism
A, exchange current and K_{ATP} current recorded in the same cardiac patch. Wortmannin (3 μM) was present in all cytoplasmic solutions. Exchange current was activated first in the absence of K^+ by applying and removing cytoplasmic Na^+ (40 mM). Then, potassium-containing (110 mM) cytoplasmic solution was applied to support outward K^+ current, and K^+ currents were activated by applying ATP (1 mM). Removal of ATP demonstrates the presence of a large K_{ATP} current. Thereafter, activation of exchange current without K^+ revealed that the exchanger was also activated by ATP. *B*, typical K_{ATP} currents in giant excised patches from HEK 293 cells expressing SUR2A and Kir6.2. Patches were excised into solution with 4 mM Mg^{2+} and channels were allowed to run down for 2 min. Thereafter, substitution of 140 mM cytoplasmic Cs^+ for K^+ revealed no K^+ current. No K^+ current was activated by application of 2 mM GTP for 45 s, indicating that PIP kinases cannot generate PIP_2 in the excised patches. Application of 2 mM ATP for 45 s activated massive K_{ATP} currents, revealed upon removing ATP, run down having a roughly 1 min time constant. The presence of 4 μM wortmannin in all solutions did not reduce the ability of ATP to activate K^+ current. *C*, PIP_2 measurements from intact murine hearts. Retrograde perfusion of wortmannin (3 μM) for 15 min had no significant effect on cardiac PIP_2 or PI(4)P ($n = 4$). Perfusion of hearts for 15 min with phenylephrine (PE; 50 μM) and carbachol (10 μM) to activate Gq-coupled pathways resulted in a significant increase of PIP_2 ($n = 4$), while simultaneous perfusion with wortmannin (3 μM) resulted in a significant decrease of PIP_2.

cytoplasmic Na^+ in the absence of K^+. The exchange current is clearly activated in comparison to the current recorded at the start of the experiment with the usual loss of exchanger inactivation.

To understand whether this outcome depended on cell type, we tested the effects of wortmannin in patches from cell lines. Again, we found that wortmannin was without effect on the activation of NCX1 and K_{ATP} channel currents by ATP. Figure 7*B* illustrates results for K_{ATP} channel currents in excised giant patches from cells expressing Kir6.2 with SUR2A (Giblin *et al.* 2002). In these experiments we verified first that GTP (2 mM) does not activate currents (Collins *et al.* 1992). This result is important because PIP5-kinases, but not PI4-kinases, utilize GTP almost as well as ATP (Loijens *et al.* 1996). The lack of effect of GTP therefore eliminates a possibility that PIP_2 is being generated from PIP, rather than from PI, and supports the idea that the activation by ATP requires PI4-kinase activity. After applying GTP for 45 s, without effect, ATP (2 mM) was applied for 45 s. ATP removal revealed that massive K^+ currents were activated during the application of ATP, and the currents decayed with a time constant of about 1 s (0.5 mM Mg^{2+} with no cytoplasmic free Ca^{2+}; C7 and X7 solutions). This is one clear difference to cardiac patches, namely the near lack of K^+ current in the presence of ATP. This difference could reflect differences in K_{ATP} channel function, or it could reflect the presence of Kir channels besides K_{ATP} channels in cardiac patches.

As described in Fig. 7*C*, we also analysed the role of type III PI4-kinases in cardiac tissue via measurements of total PIP_2 in murine hearts, carried out exactly as previously described (Nasuhoglu *et al.* 2002*a*). Perfusion of 3 μM wortmannin for 15 min causes no significant change in total PIP_2 ($n = 4$). As previously described, activation of α-receptors can cause a significant rise of PI(4)P, while PIP_2 changes remain insignificant (Nasuhoglu *et al.* 2002*a*). As described in the right data set in Fig. 7*C*, PIP_2 increases highly significantly when two Gq-coupled agonists are applied. Here, phenylephrine (50 μM) is combined with muscarinic stimulation by carbachol (10 μM) for 10 min. When the agonists are applied with 3 μM wortmannin, PIP_2 does not rise but rather falls significantly by 19%. Comparing the agonist-treated hearts and the agonist/wortmannin-treated hearts, wortmannin exposure decreases PIP_2 by 36%. From these results, we conclude that the wortmannin-sensitive synthesis of PIP_2 becomes significant only in the setting of activated Gq signalling and increased PLC activity in heart.

Cardiac overexpression of PI4KIIα

The wortmannin insensitivity of NCX1 activation in excised patches prompted us to choose a type II PI4-kinase for overexpression in hearts. Because most of the PI4KIIβ isoform is inactive in resting cells (unpublished observations J. P. Albanesi), we selected PI4KIIα, which is constitutively active, for transgenic mouse generation. Previously, we showed that both PI(4)P and PIP_2 increase with expression of this kinase in cell cultures (Nasuhoglu *et al.* 2002*b*). Figure 8*A* and *B* documents by Western-blotting and enzymatic PI kinase assay the 10-fold overexpression of PI4KIIα in hearts from PI4KIIα-positive *versus* -negative littermates. Figure 8*C* shows labelling patterns for anti-PI4KIIα and anti-myc antibodies in myocytes. In transgenic (TG) myocytes, both antibodies label perinuclear, trans-Golgi, and transverse tubule membranes. T-tubule labelling by anti-PI4KIIα was not pronounced in wild-type myocytes (WT). Figure 8*D* shows histological sections of fixed hearts stained with Masson trichrome dye. As verified with dissociated myocytes, the majority of TG myocytes were about 2-fold larger in cross-section, but some also retained normal cross-sections. Average heart weights of 6-month-old animals (0.39 ± 0.06 g) were twice those of WT animals (0.22 ± 0.01 g; $P < 0.01$). Body weights (26 ± 2 g ($n = 10$) WT *versus* 28 ± 6 g ($n = 10$) TG) and the spontaneous frequencies of isolated hearts at 35°C (185 ± 12 ($n = 3$) WT and 180 ± 15 beats min^{-1} ($n = 3$) (TG) were not significantly different. PI4-kinase activity of crude cardiac membranes was increased approximately 10-fold in TG animals, and this ratio was similar with exogenous PI (0.2 mM; Fig. 8*B*). PI(4)P and PIP_2 levels were increased by 30 and 49% ($P = 0.04$ and $P = 0.01$, see Table 2), respectively. In part, these rather small changes may be explained by an 80% increase of PI(4)P phosphatase activity (Table 2).

To test for changes of membrane cycling, we analysed uptake of transferrin, cholera toxin B subunits, and the membrane dye, AM 1-43 in WT and TG myocytes. In general, transferrin and cholera toxin B monitor clathrin-dependent and clathrin-independent endocytosis, respectively (Nichols *et al.* 2001). AM 1-43 is a hydrophobic cationic dye, similar to FM 4-64, but which can be used in fixed cells. Uptake of all markers was analysed at 5, 30 and 60 min in WT and TG myocytes whose dimensions were not significantly different. Figure 8*E* shows images of myocytes incubated for 30 min with transferrin or cholera toxin B, washed for 2 min, and then fixed. From analysis of 10 or more cells from four hearts, we detected no difference in transferrin uptake between WT and TG myocytes. Uptake of cholera toxin B subunits, however, was markedly increased. Figure 8*F* compares average cell fluorescence of WT and TG myocytes, normalized to results for TG myocytes. Apparent toxin binding *per se* was determined by incubating cells for 30 min at 4°C with cholera toxin (left bar pair). It is significantly increased in TG myocytes,

reflecting either increased membrane area or density of toxin-binding lipids. At 37°C, toxin uptake at 30 min is increased on average 3.2-fold (middle bar pair), and the amount of toxin taken up and subsequently lost during a 40 min wash is increased by 2.4-fold (right pair of bars). Uptake of AM 1-43 was increased at 5 and 30 min by 85 and 33%, respectively.

In excised giant patches from cardiac myocytes, we found no change in the rate or degree of activation of Na^+–Ca^{2+} exchange current by ATP. However, exchange currents were markedly smaller. Figure 9*A* presents results for Na^+–Ca^{2+} exchange (solutions C1 and X1), Na^+–K^+ pumps (solutions X7 and C7 with 40 mM Na^+ and 1 mM ATP), and K_{ATP} potassium currents (solutions C7 and X7). All results are related to the patch capacitance (Hilgemann & Lu, 1998). NCX1 current density with 2 mM ATP was reduced by 78%, Na^+–K^+ pump current density was reduced by 57%, and K_{ATP} current density was decreased by 48%.

Confocal images of myocytes labelled with monoclonal NCX1 antibody were then analysed. Average NCX1 labelling (i.e. fluorescence) was not significantly different. However, NCX1 labelling typically appeared more granular and disorganized in TG myocytes. A significant redistribution of NCX1 was quantified by relating NCX1 labelling of the outer sarcolemma to the average NCX1 labelling across the myocyte. Figure 9*B* illustrates our procedure. Four to six line scans were

Table 2. Analysis of PI4K11α over expression phenotype

	WT	TG	*n*
Body weight	26 ± 2 g	28 ± 6 g	10
Heart weight	0.22 ± 0.01 g	0.39 ± 0.06 g	
Heart/body (%)	0.83 ± 0.1%	1.7 ± 0.3%	
Isolated heart frequency (35°C)	185 ± 12 min^{-1}	180 ± 15 min^{-1}	3
PIP	0.46 ± 0.05%	0.60 ± 0.04%	10
PIP_2	0.41 ± 0.04%	0.61 ± 0.04%	9
PI4P-ase* (%)	100%	180%	2

PI4P phosphatase activity.

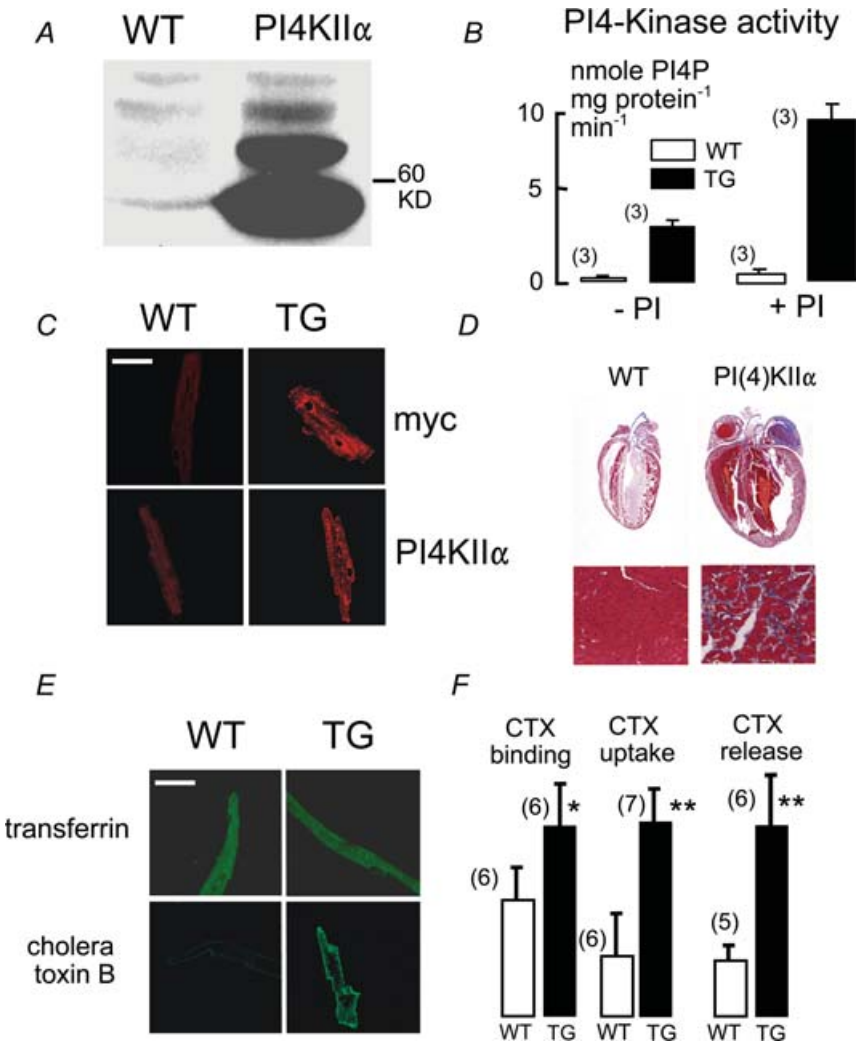

Figure 8. Overexpression of PI4KIIα in murine hearts
A, Western blots with anti-PI4KIIα of heart lysates from WT and TG mice. *B*, PI4-kinase activity in isolated membranes from WT and TG hearts, with and without 0.2 mM added phosphatidylinositol (PI). *C*, immunohistochemical verification of PI4KIIα overexpression. Labelling of TG myocytes is heavy throughout the secretory and transverse tubule membranes. *D*, typical haematoxylin-stained sections of WT and TG hearts. *E*, confocal micrographs of myocytes fixed after incubation for 30 min with labelled transferrin (20 μg ml^{-1}) or cholera toxin B subunits (0.5 μg ml^{-1}) followed by a 1 min cold wash. *F*, relative mean fluorescence of myocytes incubated with cholera toxin B subunits at 4°C for 30 min (left pair), at 37°C (middle pair), and the mean decrease of fluorescence between 5 min and 40 min after beginning wash of cholera toxin B subunits (right pair). Calibration bars in *C* and *E* correspond to 40 μm.

acquired at different myocyte positions perpendicular to the myocyte axis. Nuclear regions were excluded. Each scan was analysed, as shown in Fig. 9*B* and *C*. Average fluorescence intensities at the edges of myocytes were determined ('s' = surface), the average fluorescence between the edges was determined ('c' = centre), and a ratio (s/c) was calculated for each myocyte. Using myocytes from two WT and two TG hearts, we found that fluorescence at the edges was significantly decreased ($P < 0.01$) while fluorescence between myocyte edges was significantly increased ($P < 0.01$) in TG myocytes. Ratio of surface to central fluorescence was decreased on average by 48% ($P < 0.001$).

Discussion

Our results suggest that cardiac Na^+–Ca^{2+} exchangers are subject to two opposing influences of PIP_2, a direct

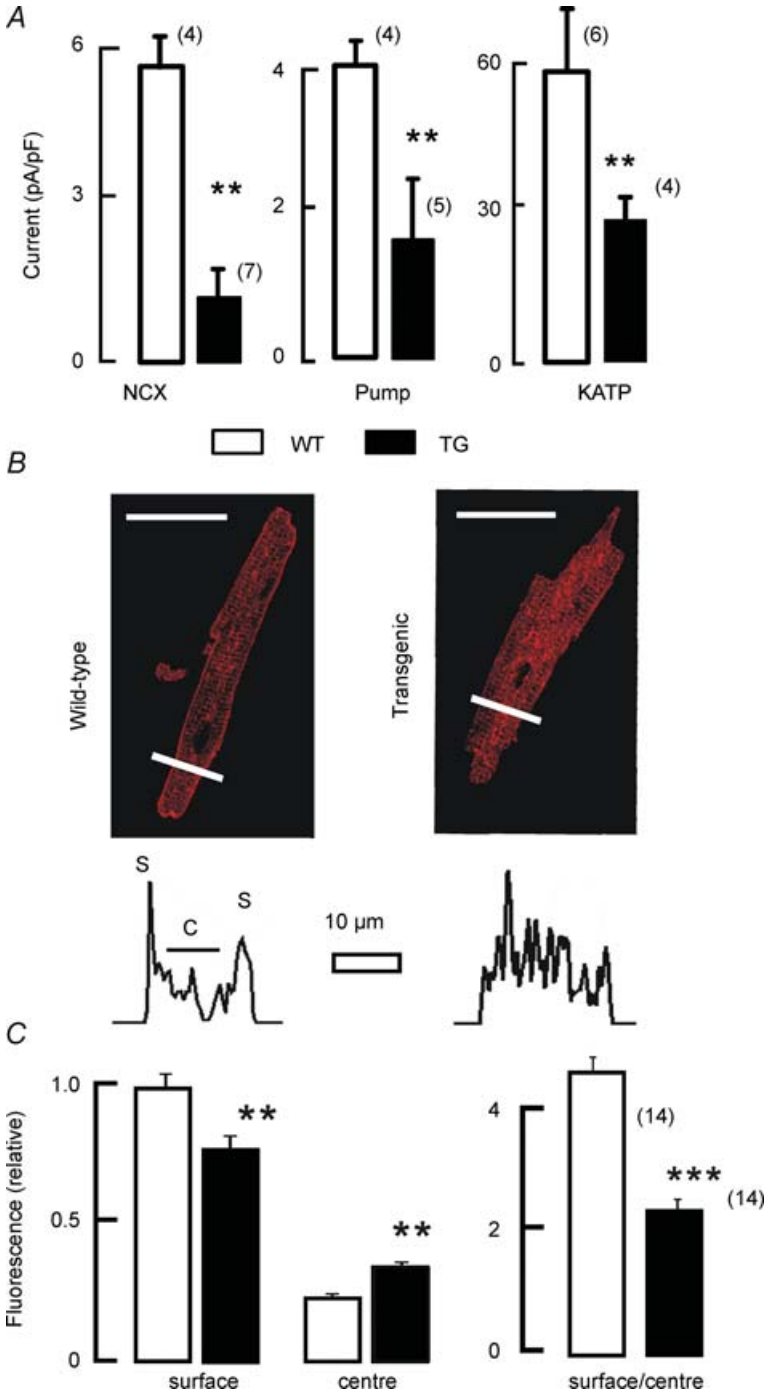

Figure 9. NCX1 currents and redistribution in TG myocytes
A, current densities of NCX1, Na^+–K^+ pumps and K_{ATP} potassium channels in giant patches excised from WT and TG myocytes. *B*, immunofluorescence staining for NCX1 in WT and TG myocytes. 's' is peak fluorescence intensity at the edge (surface) of myocytes. 'c' is average (central) fluorescence intensity between edges. Calibration bars correspond to 40 μm. *C*, composite results for the averages of 5 scans of 14 WT and 14 TG myocytes.

activating effect noted previously and at least one strong inactivating mechanism. The simplest interpretations of our data are that the NCX1 gating reactions reflect the binding and dissociation of PIP_2 from the exchanger, and that endocytosis of NCX1 underlies the indirect inhibitory effect of PIP_2 on exchange activity in intact cells. The strengths and weaknesses of these hypotheses will now be discussed.

New insights into NCX1 activation by PIP_2

The gating reactions that modulate NCX1 are functionally very complex (Hilgemann *et al.* 1992*a*,*b*). Structurally, it is now known that these reactions represent molecular interactions between the exchanger's ion transport sites, multiple Ca^{2+} binding sites in the cytoplasmic loop (Hilge *et al.* 2006; Nicoll *et al.* 2006), and the exchanger's PIP_2-binding domain (He *et al.* 2000). Because the inward exchange current, in the absence of cytoplasmic Na^+, is not affected by the gating reactions or by PIP_2 (Fig. 1*C*), PIP_2 would appear to modulate the exchanger exclusively via changes of its gating reactions. As described in Fig. 1, exogenous PIP_2 can completely overcome both Na^+-dependent inactivation and the secondary activation by cytoplasmic Ca^{2+} in cardiac patches, so that exchange activity appears to depend only on driving forces of transport. These results naturally raise a question as to how the regulatory Ca^{2+} sites are coupled with the PIP_2-binding domain. Our results would suggest that the binding of Ca^{2+} at the regulatory sites within the large cytoplasmic loop of NCX1 may exert long-range effects to increase the availability of the PIP_2-binding domain to the membrane. For the Na^+-dependent inactivation, our results suggest that the presence of Na^+ in the exchanger's transport sites has the opposite effect, namely to disengage the PIP_2-binding domain from the membrane and therewith favour inactivation by disfavouring NCX1 interaction with PIP_2.

At first, the specificity of PIP_2 to activate 'reverse' Na^+–Ca^{2+} exchange seems at odds with the fact that anionic phospholipids activate Ca^{2+} uptake by 'forward' Na^+–Ca^{2+} exchange when exchangers are reconstituted into phospholipid vesicles (Vemuri & Philipson, 1988). However, protocols used with vesicles require that vesicles are first loaded with Na^+ and thereby exposed to Na^+ on both membrane sides until they are diluted into Ca^{2+} uptake medium. Ca^{2+} uptake will be strongly influenced by the inactivation mechanisms for a few seconds after removal of Na^+ (Hilgemann *et al.* 1992*b*). As pointed out in the Introduction, anionic phospholipids besides PIP_2 might substitute for PIP_2 in intact cells. Thus, the presence of other activating lipids might explain why inhibition of outward exchange current with PIP_2 depletion by PLC activation is not an invariable finding in BHK cells with receptor overexpression (Figs 2 and 3). Both phosphatidic acid (Vemuri & Philipson, 1988; Hilgemann & Collins, 1992) and acyl CoA (Shumilina *et al.* 2006; Riedel *et al.* 2006) can have large activating effects on Na^+–Ca^{2+} exchange and K_{ATP} potassium channels. Since inhibition of outward exchange current by M1 receptors persists in the absence of cytoplasmic ATP and the presence of non-hydrolysable ATP (Fig. 3), it is unlikely that PKCs or other ATP-hydrolysing mechanisms are involved.

Possible regulation of NCX1 by cytoskeleton- and PIP_2-dependent membrane trafficking

As expected from results with excised patches, we never observed inhibition of the inward exchange current in whole-cell recording during muscarinic receptor activation. Rather, exchange current can be activated with cytoplasmic free Ca^{2+} in the range of 3–8 μM (Fig. 4). Because this activation is accompanied by an increase of cell capacitance (5–15%), it is possible that it involves membrane insertion. Phospholipase activities have long been considered to have 'fusogenic' potential (Luk *et al.* 1993). Phospholipase C activity appears to be essential in membrane fusion underlying vacuole expansion in yeast (Jun *et al.* 2004) and it appears to enhance exocytosis in mast cells (Hammond *et al.* 2006). Direct interactions of DAG, the product of PLC activity, with 'Munc' proteins may modulate and possibly facilitate regulated exocytosis (Rizo & Sudhof, 2002) and, more relevant to this study, the trafficking of transporters to the surface membrane (Khan *et al.* 2001). At the same time, a decrease of PIP_2 is expected to inhibit endocytosis (Carvou *et al.* 2006). Our experience is that an increase in capacitance and an enhancement of exchange current by receptor activation both require the presence of rather high cytoplasmic free Ca^{2+} and therefore may be related phenomena. Taken together, the results suggest that the cells employed in this study (BHK and CHO cells) can undergo Ca^{2+}-dependent fusion events, and that Gq-coupled receptor activation in the presence of high cytoplasmic Ca^{2+} can promote such events with insertion of transporters into the cell surface.

In spite of many possible artifacts, it is striking that perfusion of PIP_2 into cells can cause a rapid decrease of capacitance (5–20% of total cell area) with a loss of NCX1 activity (Fig. 5). The speed of these effects and their reversal are remarkable, if they indeed reflect membrane retrieval and insertion. From previous studies, we know that the ionic contents of small cells can be dialysed for the most part within 2–3 s using large patch pipettes (Hilgemann & Lu, 1998). It may be possible that PIP_2 first binds to the pipette wall and then diffuses laterally into the cell membrane, where it recruits and activates proteins involved in endocytosis. The open question is whether PIP_2 could insert quickly enough

into the cell membrane and be metabolized quickly enough upon removal from the pipette to account for the results.

At this time, we favour the interpretation that exchangers are indeed being inserted and retrieved from the cell surface in these experiments because effects of overexpressing lipid kinases on NCX1 are inhibitory (Figs 6 and 9) and because the fraction of exchangers that can be labelled in cells decreases (Shen *et al.* 2007) as expected. But we also have one cautionary note. In Figs 4 and 6, the ratio of current to capacitance changes are on average 61.5 ± 14 pA pF^{-1}. Maximal single exchanger currents are about 1 fA (Hilgemann, 1996), so these changes would reflect the movement of about 61 exchangers per femtofarad of membrane. Assuming a specific capacitance of 1 μF cm^{-2}, a 40 nm vesicle would correspond to 0.1 fF. Thus, six transporters would traffic per vesicle, and on first consideration this seems to be a large number.

In support of our interpretation, membrane particles that probably reflect sodium pumps and Na^+–Ca^{2+} exchangers occur in densities of about 2200 per square micrometre in cardiac sarcolemma of intact heart (Frank *et al.* 1988). The particles often appear bunched and can reversibly aggregate so that a 50 nm diameter membrane spot could readily contain 10 particles. Another factor that can support our interpretation is that compensatory membrane movements often occur during both endo- and exocytosis (Kilic *et al.* 2001), so that more membrane turnover can be substantially greater than indicated from capacitance changes. The biphasic capacitance response to M1 receptor activation (Fig. 2) is very suggestive of an increased membrane cycling. It remains to be established whether membrane cytoskeletal changes are required for the effects of depleting and increasing PIP_2 described in this article. One established mechanism, which would link the effects of changing PIP_2, membrane cytoskeleton (Fig. 4), and membrane trafficking is that depletion of PIP_2 can favour exocytosis by removing a 'filter' function of polymerized actin at the vesicle–membrane interface (Qualmann & Kessels, 2002; Schafer, 2002; Orth & McNiven, 2006).

Wortmannin and the function of PI4-kinase isoforms in excised patches and intact cells

Wortmannin is a non-specific 'ATP site' inhibitor at high concentrations, and it inhibits only one class of PI4-kinases, the type III group (Balla *et al.* 1997; Balla & Balla, 2006). Support for a 'specific' PI4-kinase-related mechanism comes from findings that wortmannin inhibits resynthesis of PIP_2 after PLC activation (Nakanishi *et al.* 1995) and that wortmannin can inhibit recovery of PIP_2-sensitive currents after PLC-dependent inhibition (Suh & Hille, 2002). In so far as the stimulation of PIP_2-activated currents by ATP reflects a PI4-kinase activity (Hilgemann & Ball, 1996), it appears problematic that wortmannin has no inhibitory effect in excised membrane patches (Fig. 7). GTP, which is used by PIP-kinases (Loijens *et al.* 1996), does not activate the PIP_2-sensitive channels and transporters in excised patches, and our original evidence for a role of PIP_2 in transporter regulation was based on effects of PI removal and replenishment in excised patches (Hilgemann & Ball, 1996). Our interpretation therefore is that the type III PI4-kinases are not normally active in the surface membrane, and that they become important mostly in the context of receptor activation. One possibility is that the type III PI4-kinases come into play only when PI starts to be depleted in the surface membrane with continued PLC activation. As membrane trafficking to the surface membrane is increased during M1 receptor activation (Fig. 2), an attractive explanation is that membrane insertion during receptor activation brings both PI and PIP to the surface membrane, as well as PI4-kinases themselves.

Overexpression of lipid kinases in cell lines and murine myocytes

Our experiments to manipulate lipid kinases by molecular biological means were encouraged by previous reports that PIP_2-sensitive potassium channels can be up-regulated by over-expressing lipid kinases (Shyng *et al.* 2000; Winks *et al.* 2005). However, we have not been able to extend those results to excised patches or to Na^+–Ca^{2+} exchange. As described in connection with Fig. 6, multiple PI4- and PIP5-kinases either had no effect or decreased exchanger current densities. In the simplest case, PIP_2 synthesis promotes endocytosis of membrane containing lipid kinases whenever a critical density of PIP_2 is exceeded.

To address these issues in intact heart, we generated mice with cardiac-specific overexpresssion of the wortmannin-insensitive PI4-kinase, type IIα. As documented in Fig. 8, active PI4KIIα was overexpressed in transgenic murine hearts by at least 10-fold, and the resulting phenotype included cardiac hypertrophy. As in cell culture experiments (Nasuhoglu *et al.* 2002*b*), overexpression elevates both PI(4)P and PIP_2 (Table 2), but the increments (30 and 48%, respectively) are rather small. Based on our analysis of transferrin and cholera toxin uptake by myocytes, the non-clathrin trafficking pathway (i.e cholera toxin pathway) is up-regulated by at least 2-fold (Fig. 8). A fundamental role of PIP5-kinases in promoting membrane turnover is well established (Galiano *et al.* 2002; Padron *et al.* 2003; Roth, 2004). It is a speculative possibility that membrane trafficking might actually contribute to the regulation of PIP_2 levels in the surface membrane, whereby an

increase of PIP_2 would cause greater dephosphorylation of PIP_2 via endocytic mechanisms. Transporters that can leave the surface membrane via trafficking would logically be affected more than constitutively anchored mechanisms, and the effect on NCX1 is largest (> 75%) among the mechanisms we have analysed (Fig. 9). From immunohistochemical analysis, there is no evidence for a decrease of the total numbers of exchangers in cells. Exchangers appear to be relocalized away from the external surface membrane (Fig. 9), possibly therefore to internal membranes.

In summary, several lines of evidence support the view that, in a cellular environment, changes of PIP_2 strongly affect NCX1 activity by both direct and indirect mechanisms. The major indirect mechanism may involve membrane trafficking, as well as changes of cytoskeleton. Multiple roles of PIP_2 metabolism in membrane trafficking are well documented in the literature, including vesicle priming on the exocytosis side (Eberhard *et al.* 1990) and recruitment of adaptors and G-proteins on the endocytosis side (Haucke, 2005). Some of our results suggest that NCX1 can be removed from the plasmalemma by PIP_2-dependent endocytosis, and some results suggest that NCX1 may be inserted in response to cleavage of PIP_2 when cytoplasmic Ca^{2+} is elevated. In this latter case, disruptions of membrane actin cytoskeleton may play a role, and such disruptions may be favoured both by high cytoplasmic Ca^{2+} and by PIP_2 depletion in the protocols we employ. While a number of results suggest that NCX1 can move into and out of the surface membrane of cell lines quite rapidly, it remains to be tested whether such movements are physiologically relevant and might be related to a suggested activation of NXC1 activity by Gq-dependent G-protein-coupled receptors in intact heart (Ballard & Schaffer, 1996; Stengl *et al.* 1998; Zhang *et al.* 2001). In the article that follows (Shen *et al.* 2007), we describe a new approach to address these issues in intact cardiac myocardium.

References

Asteggiano C, Berberian G & Beauge L (2001). Phosphatidyl inositol-4,5-bisphosphate bound to bovine cardiac Na^+/Ca^{2+} exchanger displays a MgATP regulation similar to that of the exchange fluxes. *Eur J Biochem* **268**, 437–442.

Balla A & Balla T (2006). Phosphatidylinositol 4-kinases: old enzymes with emerging functions. *Trends Cell Biol* **16**, 351–361.

Balla T, Downing GJ, Jaffe H, Kim S, Zolyomi A & Catt KJ (1997). Isolation and molecular cloning of wortmannin-sensitive bovine type III phosphatidylinositol 4-kinases. *J Biol Chem* **272**, 18358–18366.

Ballard C & Schaffer S (1996). Stimulation of the Na^+/Ca^{2+} exchanger by phenylephrine, angiotensin II and endothelin 1. *J Mol Cell Cardiol* **28**, 11–17.

Barylko B, Gerber SH, Binns DD, Grichine N, Khvotchev M, Sudhof TC, Albanesi JP (2001). A novel family of phosphatiylinosital 4–kinases conserved from yeast to humans. *J Biol Chem* **276**, 7705–7708.

Bossuyt J, Taylor BE, James-Kracke M & Hale CC (2002). Evidence for cardiac sodium–calcium exchanger association with caveolin-3. *FEBS Lett* **511**, 113–117.

Carvou N, Norden AG, Unwin RJ & Cockcroft S (2006). Signalling through phospholipase C interferes with clathrin-mediated endocytosis. *Cell Signal* **19**, 42–51.

Cavalli A, Eghbali M, Minosyan TY, Stefani E & Philipson KD (2007). Localization of sarcolemmal proteins to lipid rafts in the myocardium. *Cell Calcium*; DOI:10.1016/j.ceca.2007.01.003.

Cho H, Kim YA, Yoon JY, Lee D, Kim JH, Lee SH & Ho WK (2005). Low mobility of phosphatidylinositol 4,5-bisphosphate underlies receptor specificity of Gq-mediated ion channel regulation in atrial myocytes. *Proc Natl Acad Sci U S A* **102**, 15241–15246.

Clements GB, Fenyo EM & Klein G (1976). In vitro derived mouse A9 cell clones differing in malignancy: analysis by somatic cell hybridization with YACIR lymphoma cell clones. *Proc Natl Acad Sci U S A* **73**, 2004–2007.

Collins A, Somlyo AV & Hilgemann DW (1992). The giant cardiac membrane patch method: stimulation of outward Na^+–Ca^{2+} exchange current by MgATP. *J Physiol* **454**, 27–57.

Condrescu M & Reeves JP (2006). Actin-dependent regulation of the cardiac Na^+/Ca^{2+} exchanger. *Am J Physiol Cell Physiol* **290**, C691–C701.

Czech MP (2003). Dynamics of phosphoinositides in membrane retrieval and insertion. *Annu Rev Physiol* **65**, 791–815.

Downes CP, Gray A & Lucocq JM (2005). Probing phosphoinositide functions in signaling and membrane trafficking. *Trends Cell Biol* **15**, 259–268.

Eberhard DA, Cooper CL, Low MG & Holz RW (1990). Evidence that the inositol phospholipids are necessary for exocytosis. Loss of inositol phospholipids and inhibition of secretion in permeabilized cells caused by a bacterial phospholipase C and removal of ATP. *Biochem J* **268**, 15–25.

Egger M, Porzig H, Niggli E & Schwaller B (2005). Rapid turnover of the 'functional' Na^+-Ca^{2+} exchanger in cardiac myocytes revealed by an antisense oligodeoxynucleotide approach. *Cell Calcium* **37**, 233–243.

Frank JS, Beydler S, Wheeler N & Shine KI (1988). Myocardial sarcolemma in ischemia: a quantitative freeze-fracture study. *Am J Physiol Heart Circ Physiol* **255**, H467–H475.

Frank JS, Mottino G, Reid D, Molday RS & Philipson KD (1992). Distribution of the Na^+-Ca^{2+} exchange protein in mammalian cardiac myocytes: an immunofluorescence and immunocolloidal gold-labeling study. *J Cell Biol* **117**, 337–345.

Galiano FJ, Ulug ET & Davis JN (2002). Overexpression of murine phosphatidylinositol 4-phosphate 5-kinase type Iβ disrupts a phosphatidylinositol 4,5 bisphosphate regulated endosomal pathway. *J Cell Biochem* **85**, 131–145.

Giblin JP, Quinn K & Tinker A (2002). The cytoplasmic C-terminus of the sulfonylurea receptor is important for K_{ATP} channel function but is not key for complex assembly or trafficking. *Eur J Biochem* **269**, 5303–5313.

Grishanin RN, Kowalchyk JA, Klenchin VA, Ann K, Earles CA, Chapman ER, Gerona RR & Martin TF (2004). CAPS acts at a prefusion step in dense-core vesicle exocytosis as a PIP2 binding protein. *Neuron* **43**, 551–562.

Haley JE, Abogadie FC, Delmas P, Dayrell M, Vallis Y, Milligan G, Caulfield MP, Brown DA & Buckley NJ (1998). The α subunit of Gq contributes to muscarinic inhibition of the M-type potassium current in sympathetic neurons. *J Neurosci* **18**, 4521–4531.

Hammond GR, Dove SK, Nicol A, Pinxteren JA, Zicha D & Schiavo G (2006). Elimination of plasma membrane phosphatidylinositol (4,5)-bisphosphate is required for exocytosis from mast cells. *J Cell Sci* **119**, 2084–2094.

Haucke V (2005). Phosphoinositide regulation of clathrin-mediated endocytosis. *Biochem Soc Trans* **33**, 1285–1289.

He Z, Feng S, Tong Q, Hilgemann DW & Philipson KD (2000). Interaction of PIP_2 with the XIP region of the cardiac Na/Ca exchanger. *Am J Physiol Cell Physiol* **278**, C661–C666.

Hilge M, Aelen J & Vuister GW (2006). Ca^{2+} regulation in the Na^+/Ca^{2+} exchanger involves two markedly different Ca^{2+} sensors. *Mol Cell* **22**, 15–25.

Hilgemann DW (1996). Unitary cardiac Na^+,Ca^{2+} exchange current magnitudes determined from channel-like noise and charge movements of ion transport. *Biophys J* **71**, 759–768.

Hilgemann DW & Ball R (1996). Regulation of cardiac Na^+,Ca^{2+} exchange and K_{ATP} potassium channels by PIP_2. *Science* **273**, 956–959.

Hilgemann DW & Collins A (1992). Mechanism of cardiac Na^+–Ca^{2+} exchange current stimulation by MgATP: possible involvement of aminophospholipid translocase. *J Physiol* **454**, 59–82.

Hilgemann DW, Collins A & Matsuoka S (1992*a*). Steady-state and dynamic properties of cardiac sodium-calcium exchange. Secondary modulation by cytoplasmic calcium and ATP. *J Gen Physiol* **100**, 933–961.

Hilgemann DW, Feng S & Nasuhoglu C (2001). The complex and intriguing lives of PIP_2 with ion channels and transporters. *Sci STKE* **2001**, RE19.

Hilgemann DW & Lu CC (1998). Giant membrane patches: improvements and applications. *Meth Enzymol* **293**, 267–280.

Hilgemann DW, Matsuoka S, Nagel GA & Collins A (1992*b*). Steady-state and dynamic properties of cardiac sodium-calcium exchange. Sodium-dependent inactivation. *J Gen Physiol* **100**, 905–932.

Horowitz LF, Hirdes W, Suh BC, Hilgemann DW, Mackie K & Hille B (2005). Phospholipase C in living cells: activation, inhibition, Ca^{2+} requirement, and regulation of M current. *J Gen Physiol* **126**, 243–262.

Iwamoto T, Pan Y, Nakamura TY, Wakabayashi S & Shigekawa M (1998). Protein kinase C-dependent regulation of Na^+/Ca^{2+} exchanger isoforms NCX1 and NCX3 does not require their direct phosphorylation. *Biochemistry* **37**, 17230–17238.

Jun Y, Fratti RA & Wickner W (2004). Diacylglycerol and its formation by phospholipase C regulate Rab- and SNARE-dependent yeast vacuole fusion. *J Biol Chem* **279**, 53186–53195.

Khan AH, Thurmond DC, Yang C, Ceresa BP, Sigmund CD & Pessin JE (2001). Munc18c regulates insulin-stimulated GLUT4 translocation to the transverse tubules in skeletal muscle. *J Biol Chem* **276**, 4063–4069.

Kilic G, Angleson JK, Cochilla AJ, Nussinovitch I & Betz WJ (2001). Sustained stimulation of exocytosis triggers continuous membrane retrieval in rat pituitary somatotrophs. *J Physiol* **532**, 771–783.

Li ZP, Burke EP, Frank JS, Bennett V & Philipson KD (1993). The cardiac Na^+-Ca^{2+} exchanger binds to the cytoskeletal protein ankyrin. *J Biol Chem* **268**, 11489–11491.

Linck B, Qiu Z, He Z, Tong Q, Hilgemann DW & Philipson KD (1998). Functional comparison of the three isoforms of the Na^+/Ca^{2+} exchanger (NCX1, NCX2, NCX3). *Am J Physiol Cell Physiol* **274**, C415–C423.

Loijens JC, Boronenkov IV, Parker GJ & Anderson RA (1996). The phosphatidylinositol 4-phosphate 5-kinase family. *Adv Enzyme Regul* **36**, 115–140.

Lu CC, Kabakov A, Markin VS, Mager S, Frazier GA & Hilgemann DW (1995). Membrane transport mechanisms probed by capacitance measurements with megahertz voltage clamp. *Proc Natl Acad Sci U S A* **92**, 11220–11224.

Luk AS, Kaler EW & Lee SP (1993). Phospholipase C-induced aggregation and fusion of cholesterol-lecithin small unilamellar vesicles. *Biochemistry* **32**, 6965–6973.

Milosevic I, Sorensen JB, Lang T, Krauss M, Nagy G, Haucke V, Jahn R & Neher E (2005). Plasmalemmal phosphatidylinositol-4,5-bisphosphate level regulates the releasable vesicle pool size in chromaffin cells. *J Neurosci* **25**, 2557–2565.

Mohler PJ, Davis JQ & Bennett V (2005). Ankyrin-B coordinates the Na/K ATPase, Na/Ca exchanger, and $InsP_3$ receptor in a cardiac T-tubule/SR microdomain. *PLoS Biol* **3**, e423.

Morris JB, Huynh H, Vasilevski O & Woodcock EA (2006). α1-Adrenergic receptor signaling is localized to caveolae in neonatal rat cardiomyocytes. *J Mol Cell Cardiol* **41**, 17–25.

Nakanishi S, Catt KJ & Balla T (1995). A wortmannin-sensitive phosphatidylinositol 4-kinase that regulates hormone-sensitive pools of inositolphospholipids. *Proc Natl Acad Sci U S A* **92**, 5317–5321.

Nasuhoglu C, Feng S, Mao Y, Shammat I, Yamamato M, Earnest S, Lemmon M & Hilgemann DW (2002*a*). Modulation of cardiac PIP_2 by cardioactive hormones and other physiologically relevant interventions. *Am J Physiol Cell Physiol* **283**, C223–C234.

Nasuhoglu C, Feng S, Mao J, Yamamoto M, Yin HL, Earnest S, Barylko B, Albanesi JP & Hilgemann DW (2002*b*). Nonradioactive analysis of phosphatidylinositides and other anionic phospholipids by anion-exchange high-performance liquid chromatography with suppressed conductivity detection. *Anal Biochem* **301**, 243–254.

Nichols BJ, Kenworthy AK, Polishchuk RS, Lodge R, Roberts TH, Hirschberg K, Phair RD & Lippincott-Schwartz J (2001). Rapid cycling of lipid raft markers between the cell surface and Golgi complex. *J Cell Biol* **153**, 529–541.

Nicoll DA, Sawaya MR, Kwon S, Cascio D, Philipson KD & Abramson J (2006). The crystal structure of the primary Ca^{2+} sensor of the Na^+/Ca^{2+} exchanger reveals a novel Ca^{2+} binding motif. *J Biol Chem* **281**, 21577–21581.

O'Connell TD, Ni YG, Lin K-M, Han H & Yan Z (2003). Isolation and culture of adult mouse cardiac myocytes for signaling studies. *AfCS Research Reports* [online]. Vol. 1, no. 5. Available from http://www.signaling-gateway.org/reports/v1/CM0005/CM0005.htm

Orth JD & McNiven MA (2003). Get off my back! Rapid receptor internalization through circular dorsal ruffles. *Cancer Res* **66**, 11094–11096.

Padron D, Wang YJ, Yamamoto M, Yin H & Roth MG (2003). Phosphatidylinositol phosphate 5-kinase Iβ recruits AP-2 to the plasma membrane and regulates rates of constitutive endocytosis. *J Cell Biol* **162**, 693–701.

Qualmann B & Kessels MM (2002). Endocytosis and the cytoskeleton. *Int Rev Cytol* **220**, 93–144.

Ramos-Castaneda J, Park YN, Liu M, Hauser K, Rudolph H, Shull GE, Jonkman MF, Mori K, Ikeda S, Ogawa H & Arvan P (2005). Deficiency of ATP2C1, a Golgi ion pump, induces secretory pathway defects in endoplasmic reticulum (ER)-associated degradation and sensitivity to ER stress. *J Biol Chem* **280**, 9467–9473.

Raucher D, Stauffer T, Chen W, Shen K, Guo S, York JD, Sheetz MP & Meyer T (2000). Phosphatidylinositol 4,5-bisphosphate functions as a second messenger that regulates cytoskeleton-plasma membrane adhesion. *Cell* **100**, 221–228.

Riedel MJ, Baczko I, Searle GJ, Webster N, Fercho M, Jones L, Lang J, Lytton J, Dyck JR & Light PE (2006). Metabolic regulation of sodium-calcium exchange by intracellular acyl CoAs. *EMBO J* **25**, 4605–4614.

Rizo J & Sudhof TC (2002). Snares and Munc18 in synaptic vesicle fusion. *Nat Rev Neurosci* **3**, 641–653.

Roth MG (2004). Phosphoinositides in constitutive membrane traffic. *Physiol Rev* **84**, 699–730.

Rothermel BA, McKinsey TA, Vega RB, Nicol RL, Mammen P, Yang J, Antos CL, Shelton JM, Bassel-Duby R, Olson EN & Williams RS (2001). Myocyte-enriched calcineurin-interacting protein, MCIP1, inhibits cardiac hypertrophy in vivo. *Proc Natl Acad Sci U S A* **98**, 3328–3333.

Schafer DA (2002). Coupling actin dynamics and membrane dynamics during endocytosis. *Curr Opin Cell Biol* **14**, 76–81.

Selyanko AA, Hadley JK, Wood IC, Abogadie FC, Jentsch TJ & Brown DA (2000). Inhibition of KCNQ1–4 potassium channels expressed in mammalian cells via M_1 muscarinic acetylcholine receptors. *J Physiol* **522**, 349–355.

Shen C, Lin M-J, Yaradanakul A, Lariccia V, Hill JA & Hilgemann DW (2007). Dual control of cardiac Na^+–Ca^{2+} exchange by PIP_2: analysis of the surface membrane fraction by extracellular cysteine PEGylation. *J Physiol* **XXX**, xxx–xxx.

Shumilina E, Klocker N, Korniychuk G, Rapedius M, Lang F & Baukrowitz T (2006). Cytoplasmic accumulation of long-chain coenzyme A esters activates K_{ATP} and inhibits Kir2.1 channels. *J Physiol* **575**, 433–442.

Shyng SL, Barbieri A, Gumusboga A, Cukras C, Pike L, Davis JN, Stahl PD & Nichols CG (2000). Modulation of nucleotide sensitivity of ATP-sensitive potassium channels by phosphatidylinositol-4-phosphate 5-kinase. *Proc Natl Acad Sci U S A* **97**, 937–941.

Smrcka AV, Hepler JR, Brown KO & Sternweis PC (1991). Regulation of polyphosphoinositide-specific phospholipase C activity by purified Gq. *Science* **251**, 804–807.

Soom M, Schonherr R, Kubo Y, Kirsch C, Klinger R & Heinemann SH (2001). Multiple PIP_2 binding sites in Kir2.1 inwardly rectifying potassium channels. *FEBS Lett* **490**, 49–53.

Stauffer TP, Ahn S & Meyer T (1998). Receptor-induced transient reduction in plasma membrane PtdIns (4,5)P_2 concentration monitored in living cells. *Curr Biol* **8**, 343–346.

Stengl M, Mubagwa K, Carmeliet E & Flameng W (1998). Phenylephrine-induced stimulation of Na^+/Ca^{2+} exchange in rat ventricular myocytes. *Cardiovasc Res* **38**, 703–710.

Suh BC & Hille B (2002). Recovery from muscarinic modulation of M current channels requires phosphatidylinositol 4,5-bisphosphate synthesis. *Neuron* **35**, 507–520.

Suh BC & Hille B (2005). Regulation of ion channels by phosphatidylinositol 4,5-bisphosphate. *Curr Opin Neurobiol* **15**, 370–378.

Tolias KF & Cantley LC (1999). Pathways for phosphoinositide synthesis. *Chem Phys Lipids* **98**, 69–77.

Van BK, Dode L, Vanoevelen J, Callewaert G, De SH, Missiaen L, Parys JB, Raeymaekers L & Wuytack F (2004). The Ca^{2+}/Mn^{2+} pumps in the Golgi apparatus. *Biochim Biophys Acta* **1742**, 103–112.

Vanoevelen J, Dode L, Van BK, Fairclough RJ, Missiaen L, Raeymaekers L & Wuytack F (2005). The secretory pathway Ca^{2+}/Mn^{2+}-ATPase 2 is a Golgi-localized pump with high affinity for Ca_{2+} ions. *J Biol Chem* **280**, 22800–22808.

Vemuri R & Philipson KD (1988). Phospholipid composition modulates the Na^+-Ca^{2+} exchange activity of cardiac sarcolemma in reconstituted vesicles. *Biochim Biophys Acta* **937**, 258–268.

Wang YJ, Wang J, Sun HQ, Martinez M, Sun YX, Macia E, Kirchhausen T, Albanesi JP, Roth MG & Yin HL (2003). Phosphatidylinositol 4 phosphate regulates targeting of clathrin adaptor AP-1 complexes to the Golgi. *Cell* **114**, 299–310.

Winks JS, Hughes S, Filippov AK, Tatulian L, Abogadie FC, Brown DA & Marsh SJ (2005). Relationship between membrane phosphatidylinositol-4,5-bisphosphate and receptor-mediated inhibition of native neuronal M channels. *J Neurosci* **25**, 3400–3413.

Yin HL & Janmey PA (2003). Phosphoinositide regulation of the actin cytoskeleton. *Annu Rev Physiol* **65**, 761–789.

Zhang XQ, Ahlers BA, Tucker AL, Song J, Wang J, Moorman JR, Mounsey JP, Carl LL, Rothblum LI & Cheung JY (2006). Phospholemman inhibition of the cardiac Na^+/Ca^{2+} exchanger. Role of phosphorylation. *J Biol Chem* **281**, 7784–7792.

Zhang YH, James AF & Hancox JC (2001). Regulation by endothelin-1 of Na^+-Ca^{2+} exchange current (I_{NaCa}) from guinea-pig isolated ventricular myocytes. *Cell Calcium* **30**, 351–360.

Acknowledgements

We thank Kenneth D. Philipson (UCLA, Los Angeles) for reagents, cell lines and critical discussion. We thank Mark Shapiro (UTSA, San Antonio) and Andrew Tinker (University College London) for cell lines and constructs, and Ying-Jie Wang (UTSouthwestern, Dallas) and John P. Reeves (UMDNJ, Newark) for advice. This work was supported by NIH grants HL0679420 and HL051323 to D.W.H.